Cosmic ray acceleration and transport

Christoph Pfrommer[1]

in collaboration with

PhD students: T. Thomas[1], M. Pais[1], G. Winner[1]
K. Ehlert[1], R. Lemmerz[1], M. Werhahn[1]
Postdocs: T. Berlok[1], T. Buck[1], P. Girichidis[1], M. Shalaby[1]
E. Puchwein[1], R. Pakmor[2], V. Springel[2], T. Enßlin[2], C. Simpson[3]

[1]AIP Potsdam, [2]MPA Garching, [3]U of Chicago

Astroparticle Seminar, DESY, Zeuthen, Jan 2021

Outline

Shock waves

shock waves: sudden change in density, temperature, and pressure that decelerates supersonic flow.

thickness $\sim$ mean free path λ_{mfp}

in air, $\lambda_{mfp} \sim \mu$m,
on Earth, most shocks are mediated by collisions.

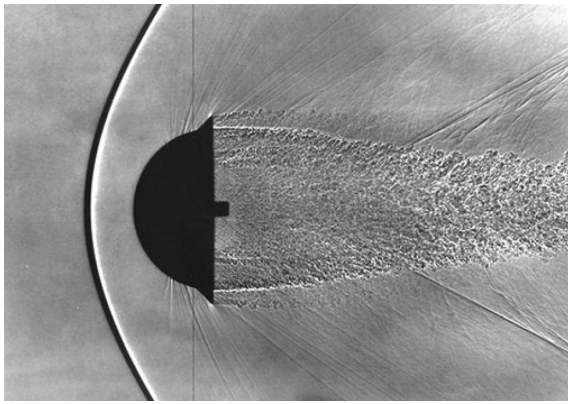

slide concept Spitkovsky

Shock waves

shock waves: sudden change in density, temperature, and pressure that decelerates supersonic flow.

thickness $\sim$ mean free path λ_{mfp}

in air, $\lambda_{\mathrm{mfp}} \sim \mu\mathrm{m}$,
on Earth, most shocks are mediated by collisions.

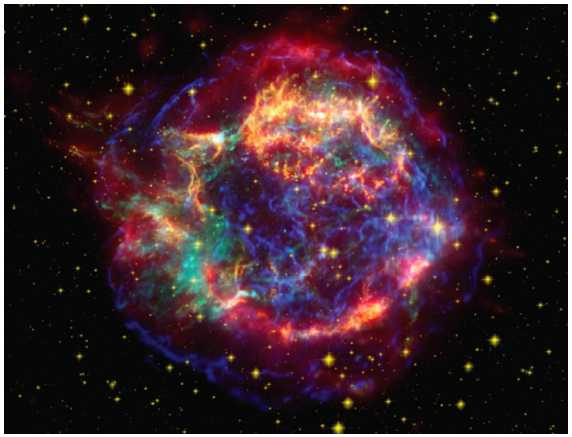

clusters/galaxies, Coulomb collisions set λ_{mfp}:

$\lambda_{\mathrm{mfp}} \sim L_{\mathrm{cluster}}/10, \qquad \lambda_{\mathrm{mfp}} \sim L_{\mathrm{SNR}}$

Mean free path $\gg$ observed shock width!

$\rightarrow$ shocks must be mediated without collisions, but through interactions with collective fields
$\rightarrow$ collisionless shocks

slide concept Spitkovsky

AIP

Particle acceleration at relativistic shock, $B_0 = 0$

- self-generated magnetic turbulence scatters particles across the shock
- each crossing results in energy gain – Fermi process
- movie below shows magnetic filaments in the shock frame (top), particle energy is measured the downstream frame (bottom): particle gains energy upon scattering in the upstream (Spitkovsky 2008)

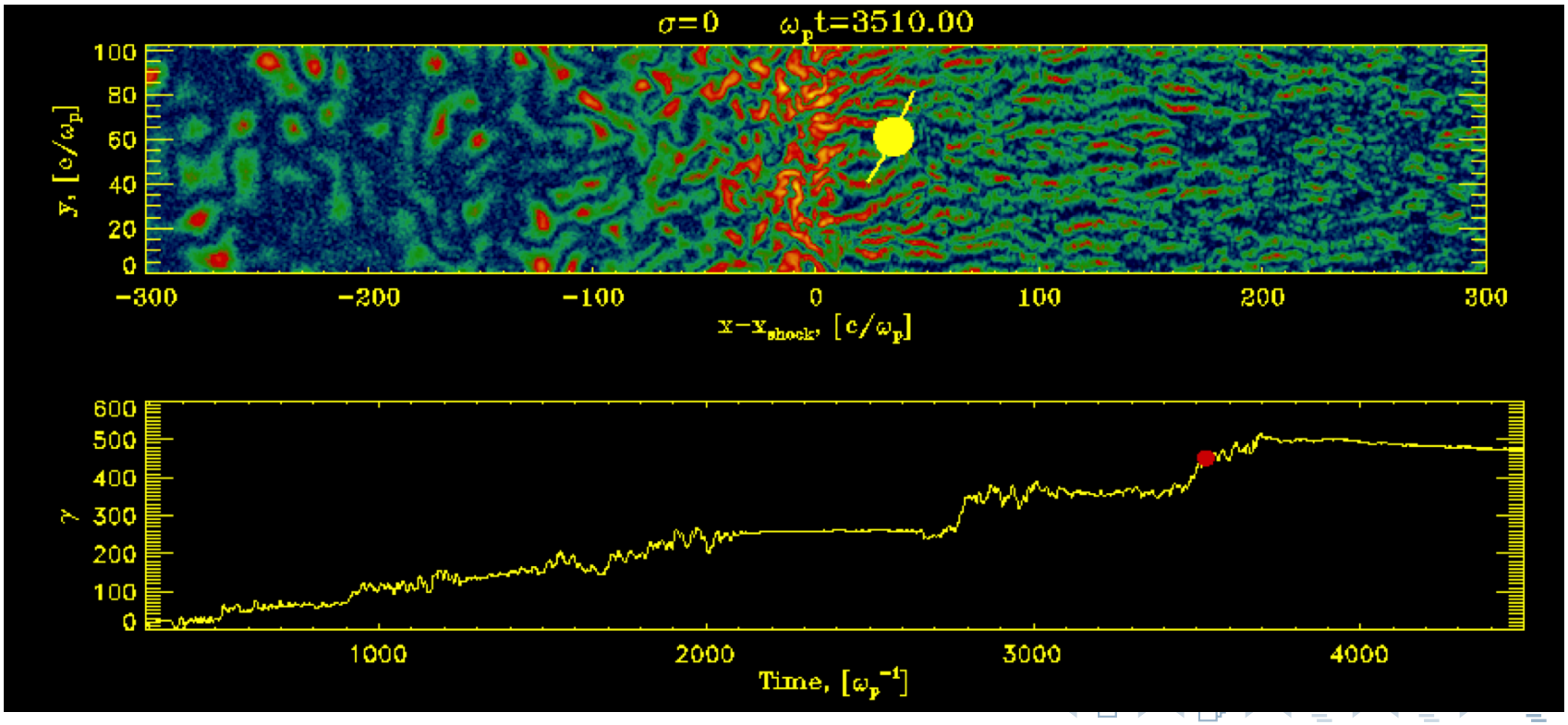

Ion spectrum

Non-relativistic parallel shock in long-term hybrid simulation

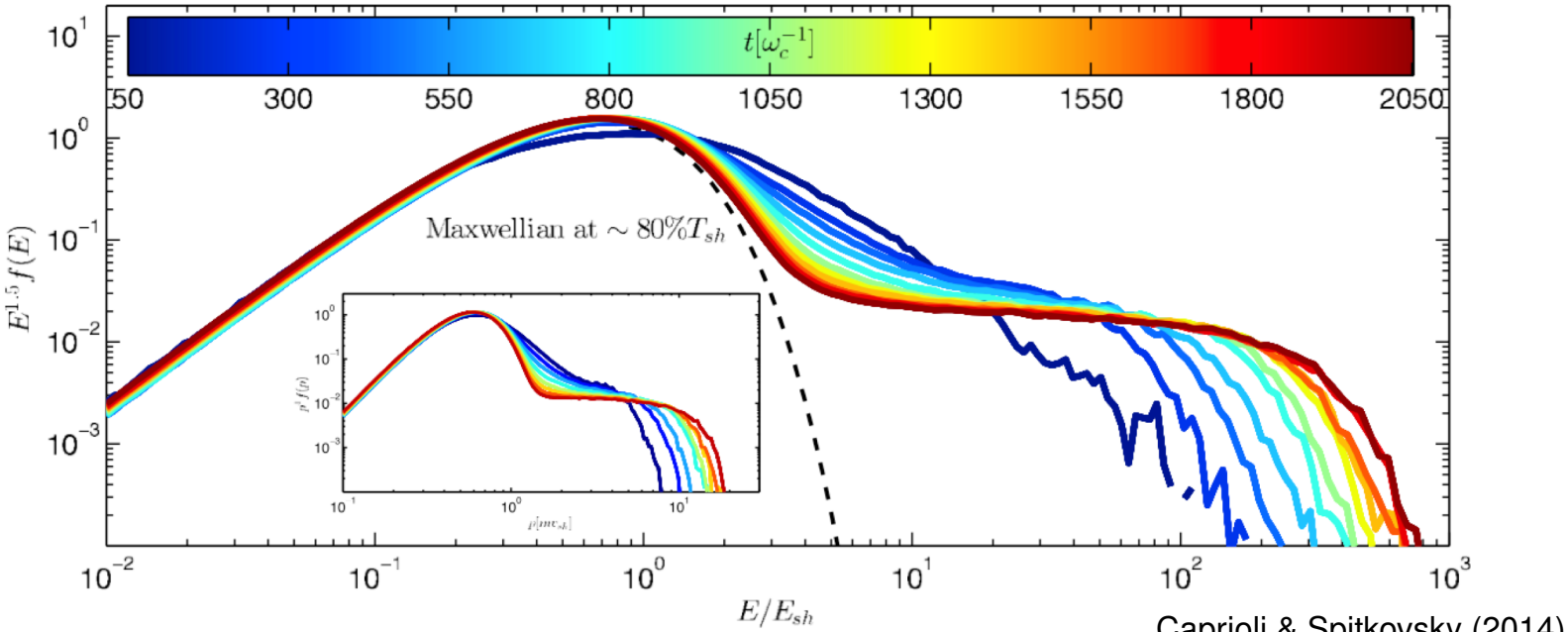

Caprioli & Spitkovsky (2014)

- quasi-parallel shocks accelerate ions
- particles gain energy in each crossing and have probability of leaving the Fermi cycle by being swept downstream → power-law spectrum
- maximum energy increases with time

Astrophysical shocks

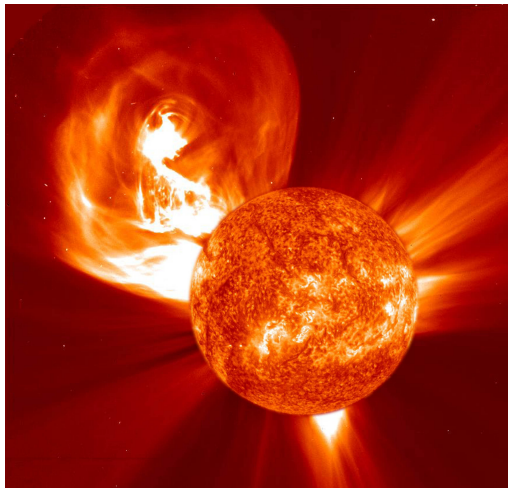

solar system shocks $\sim R_\odot$
coronal mass ejection (SOHO)

interstellar shocks ~ 20 pc
supernova 1006 (CXC/Hughes)

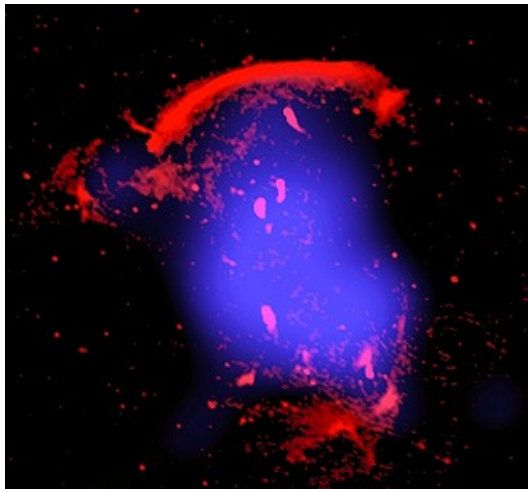

cluster shocks ~ 2 Mpc
giant radio relic (van Weeren)

AIP

Astrophysical shocks

astrophysical collisionless shocks can:

- accelerate particles (electrons and ions) $\rightarrow$ cosmic rays (CRs)
- amplify magnetic fields (or generate them from scratch)
- exchange energy between electrons and ions

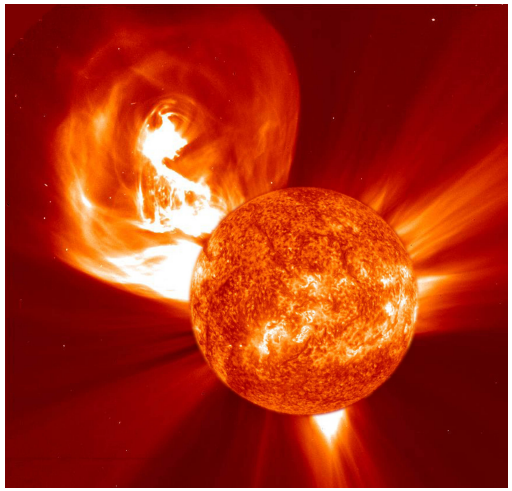

solar system shocks $\sim R_\odot$
coronal mass ejection (SOHO)

interstellar shocks $\sim$ 20 pc
supernova 1006 (CXC/Hughes)

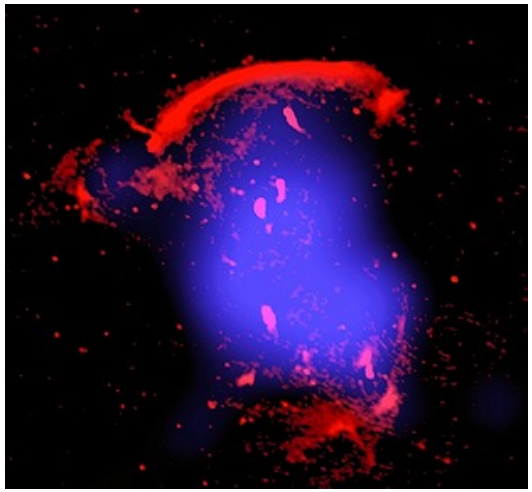

cluster shocks $\sim$ 2 Mpc
giant radio relic (van Weeren)

AIP

Astrophysical shocks

astrophysical collisionless shocks can:

- accelerate particles (electrons and ions) $\rightarrow$ cosmic rays (CRs)
- amplify magnetic fields (or generate them from scratch)
- exchange energy between electrons and ions

collisionless shocks $\Longleftrightarrow$ energetic particles $\Longleftrightarrow$ electro-magnetic waves

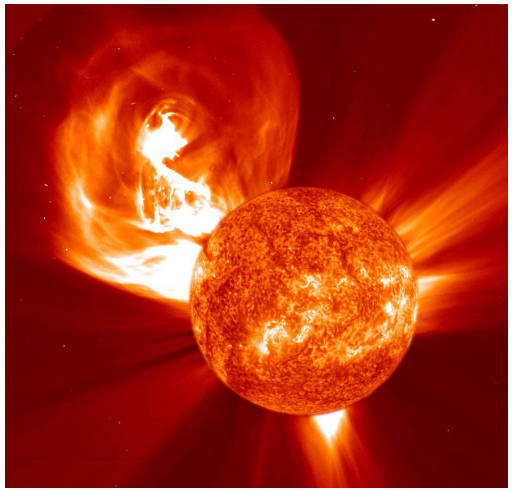

solar system shocks $\sim R_\odot$
coronal mass ejection (SOHO)

interstellar shocks $\sim$ 20 pc
supernova 1006 (CXC/Hughes)

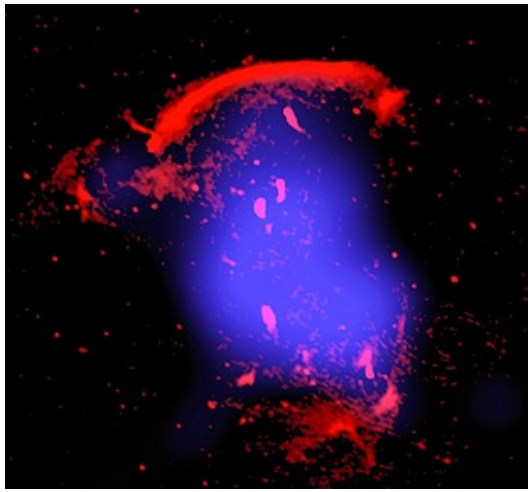

cluster shocks $\sim$ 2 Mpc
giant radio relic (van Weeren)

Global MHD simulations of SNRs with CR physics

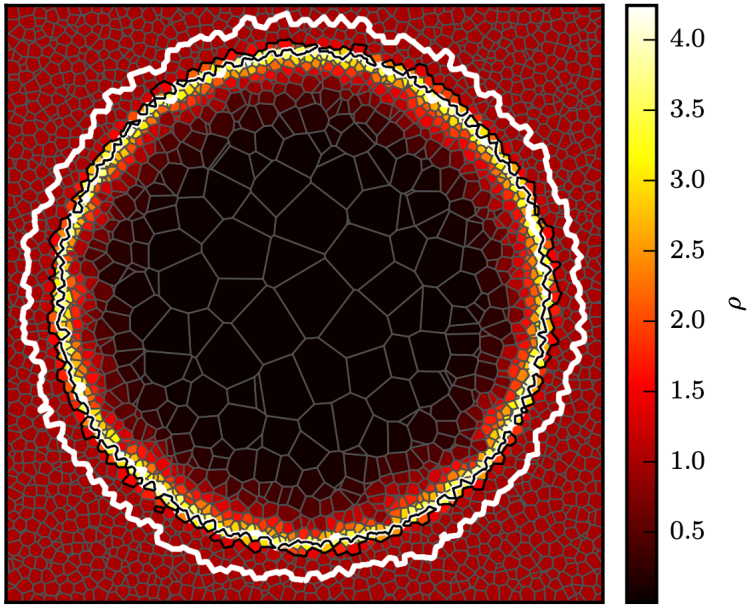

- detect and characterize shocks and jump conditions on the fly

Mach number finder

CP+ (2017) based on Schaal & Springel (2015)

Global MHD simulations of SNRs with CR physics

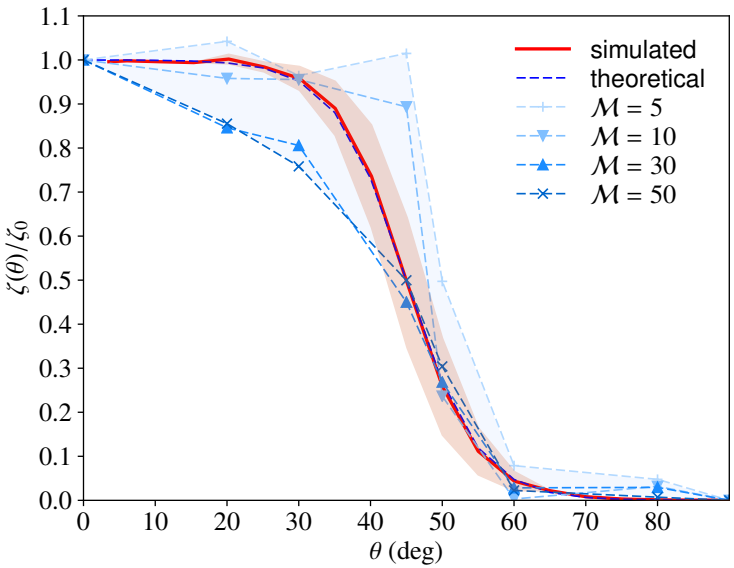

obliquity-dep. acceleration efficiency

Pais, CP+ (2018) based on
hybrid PIC sim.'s by Caprioli & Spitkovsky (2015)

- detect and characterize shocks and jump conditions on the fly
- measure Mach number $\mathcal{M}$ and magnetic obliquity θ_B

AIP

Global MHD simulations of SNRs with CR physics

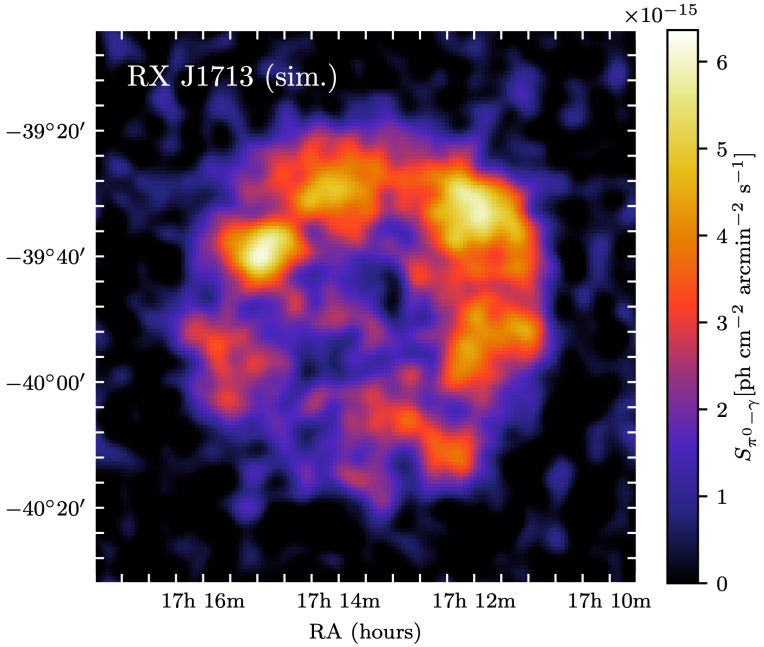

simulated TeV gamma-ray map

Pais & CP (2020)

- detect and characterize shocks and jump conditions on the fly
- measure Mach number $\mathcal{M}$ and magnetic obliquity θ_B
- inject and transport CR protons $\Rightarrow$ dynamical back reaction on gas flow, hadronic emission

AIP

Global MHD simulations of SNRs with CR physics

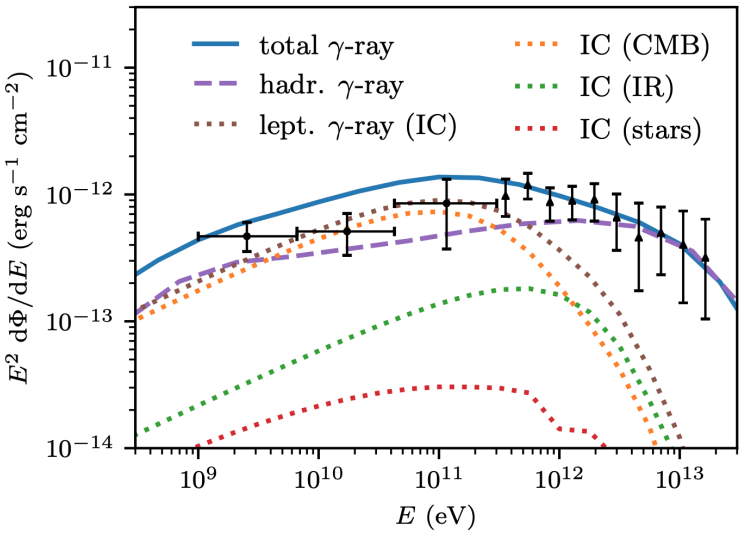

simulated gamma-ray spectrum

Winner, CP+ (2020)

- detect and characterize shocks and jump conditions on the fly
- measure Mach number $\mathcal{M}$ and magnetic obliquity θ_B
- inject and transport CR protons $\Rightarrow$ dynamical back reaction on gas flow, hadronic emission
- inject and transport CR electrons
- calculate non-thermal radio, X-ray, γ-ray emission

Cosmological moving-mesh code AREPO (Springel 2010)

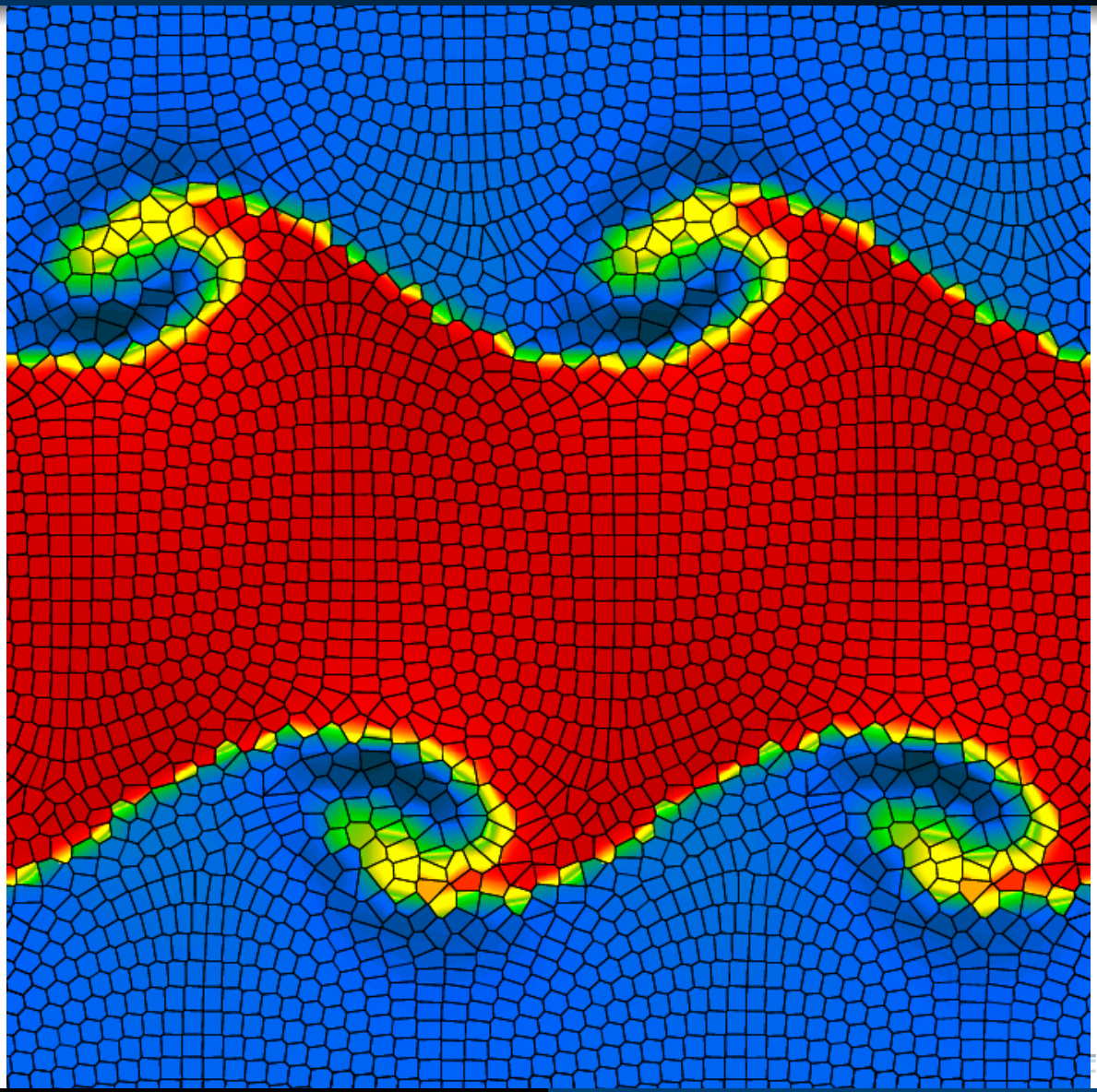

AIP

Sedov explosion

density

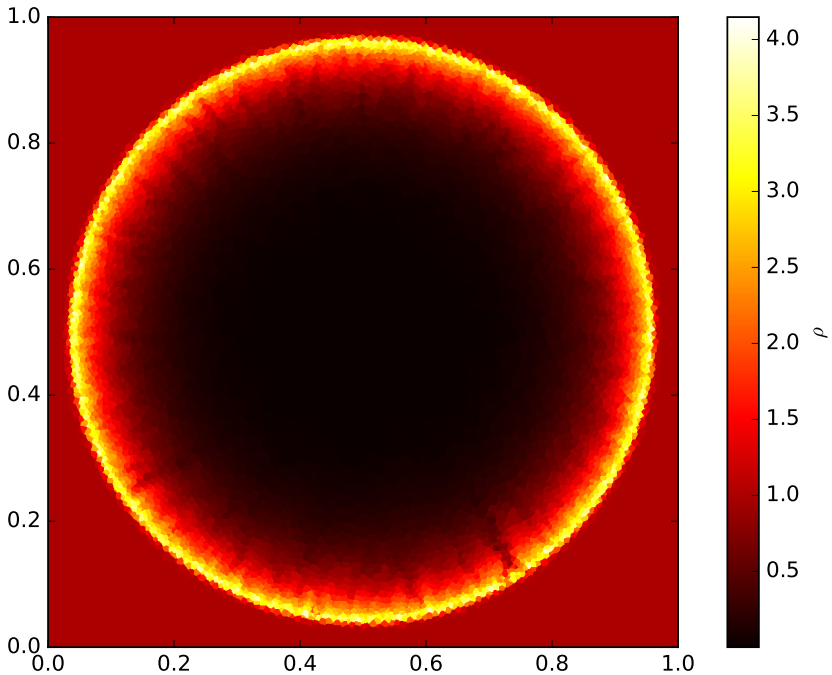

specific thermal energy

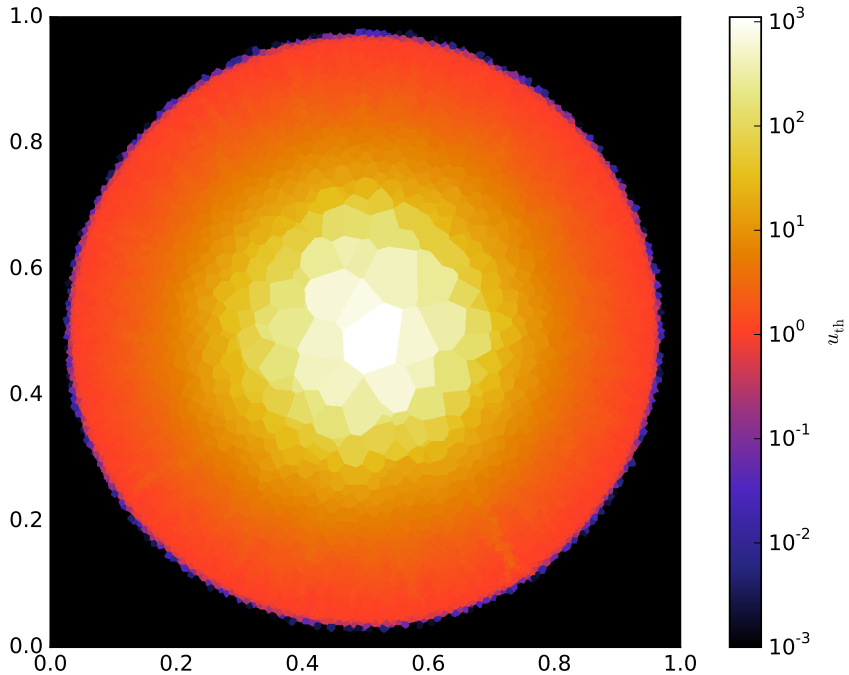

CP+ (2017)

AIP

Sedov explosion with CR acceleration

density

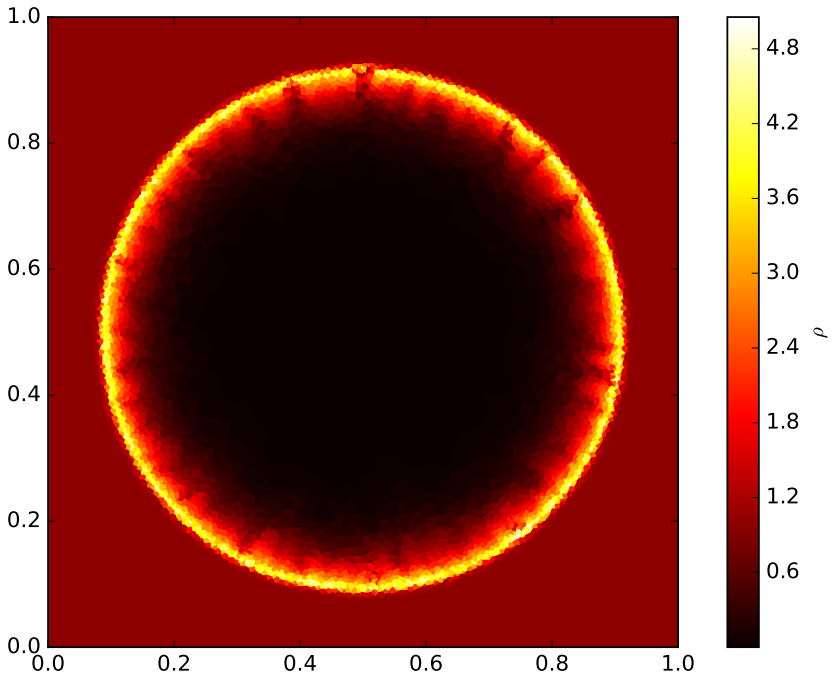

specific cosmic ray energy

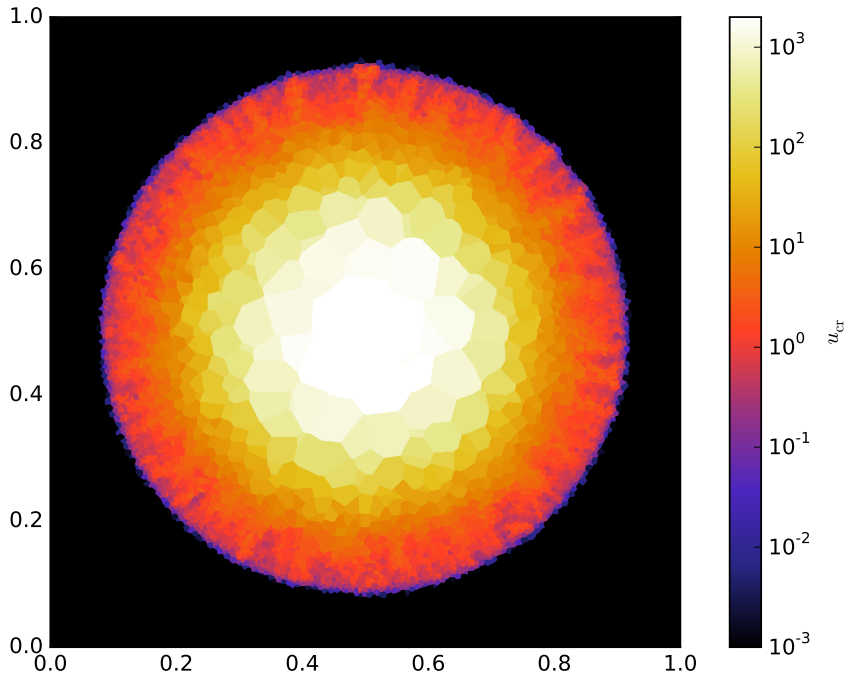

CP+ (2017)

Sedov explosion with CR acceleration

adiabatic index

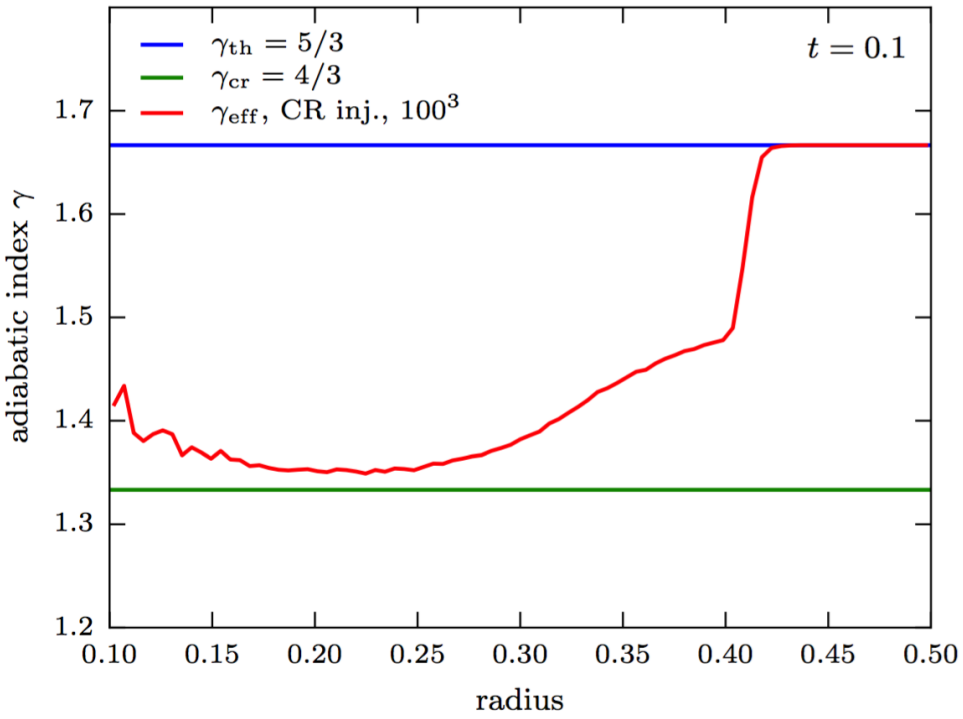

shock evolution

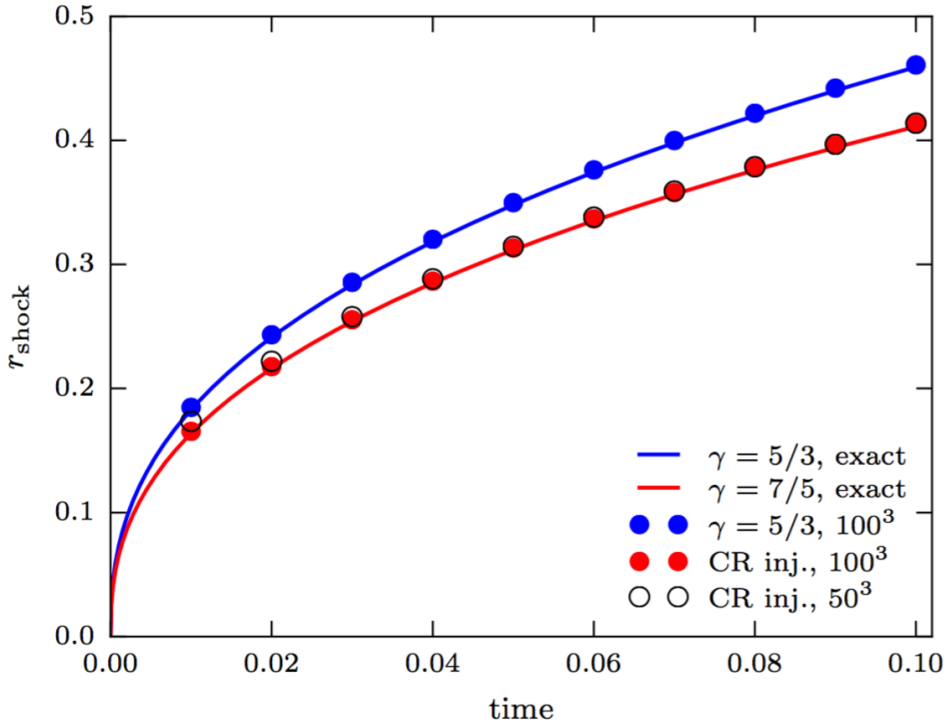

CP+ (2017)

Sedov explosion with CR acceleration

density

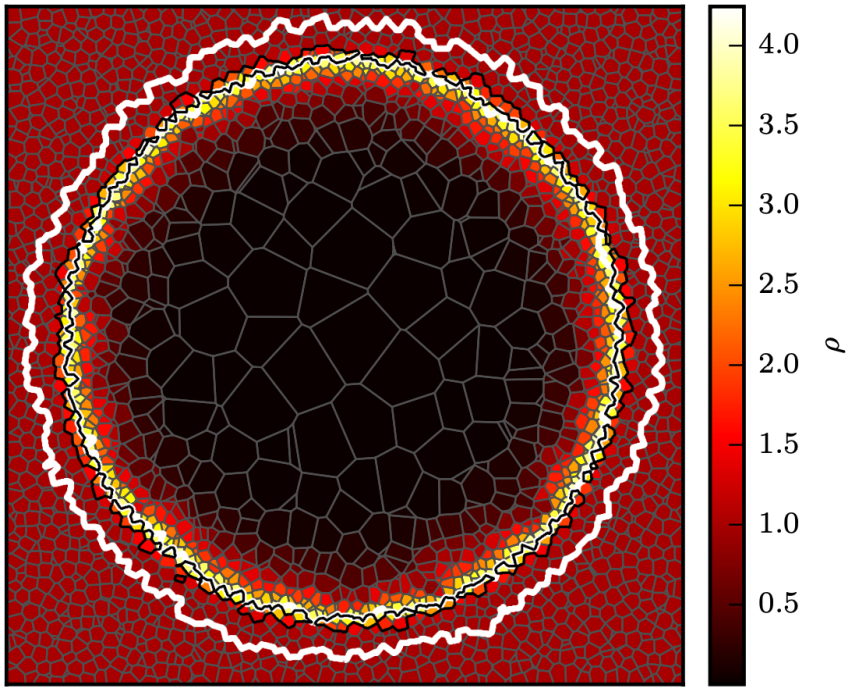

specific cosmic ray energy

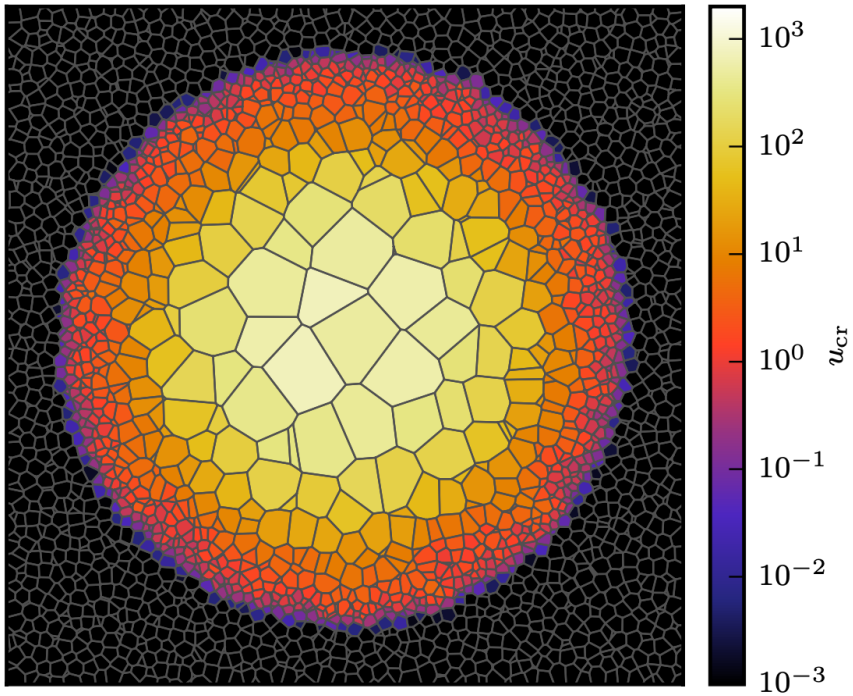

CP+ (2017)

Simulating obliquity-dependent CR proton acceleration

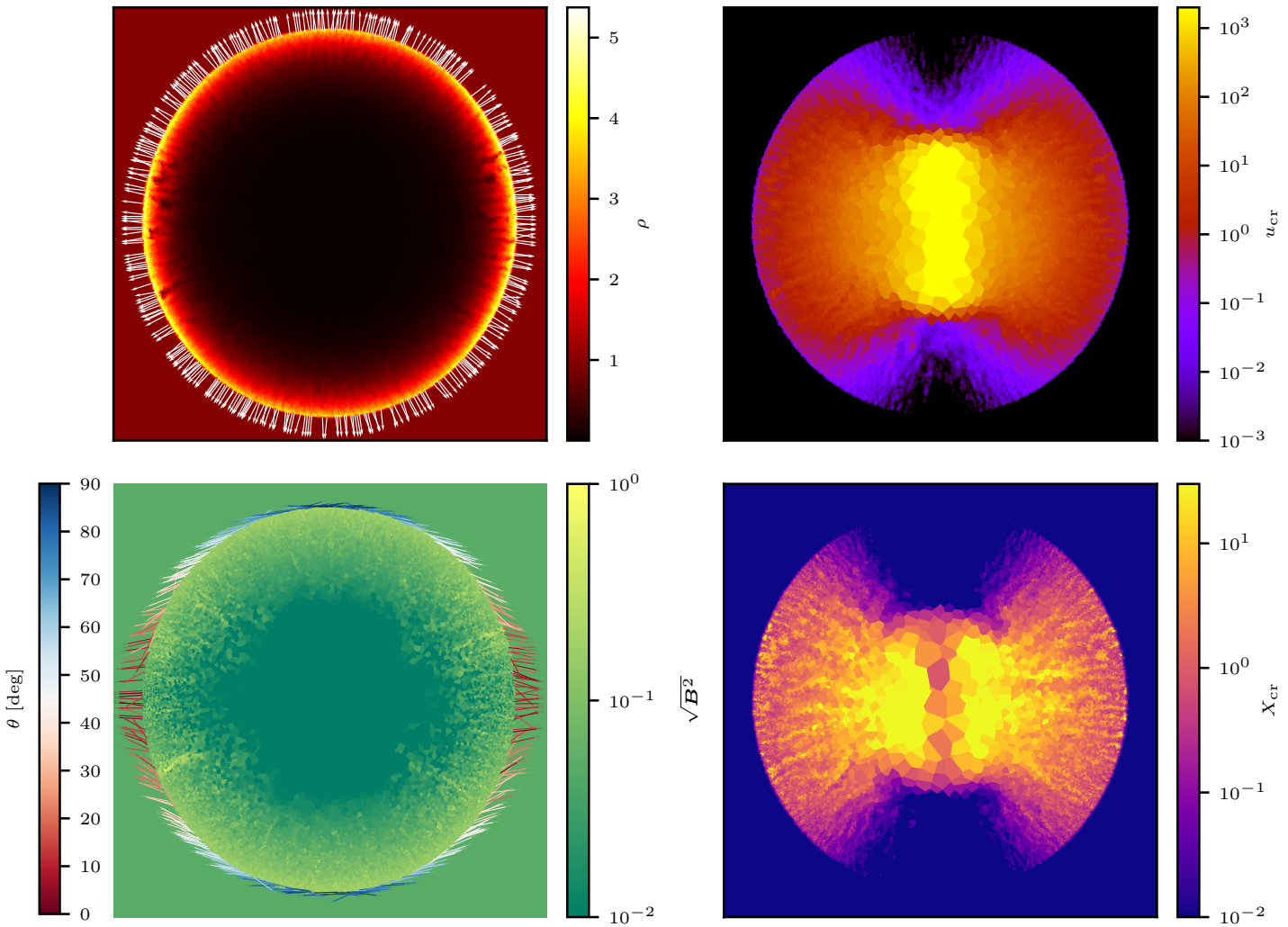

Pais, CP+ (2018)

Hadronic TeV γ rays: SN 1006

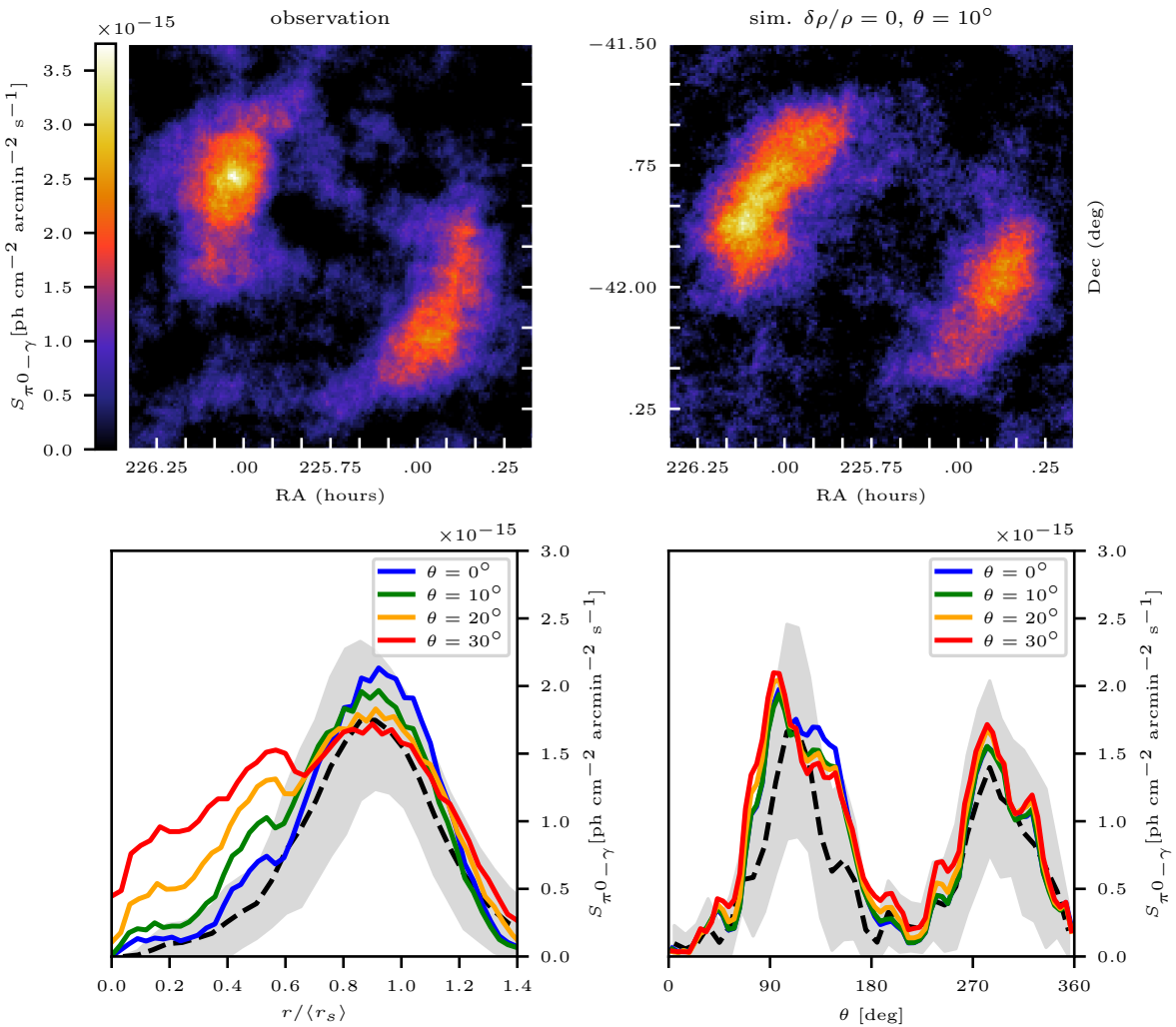

Pais & CP (2020)

Hadronic TeV γ rays: Vela Jr. and RXJ 1713

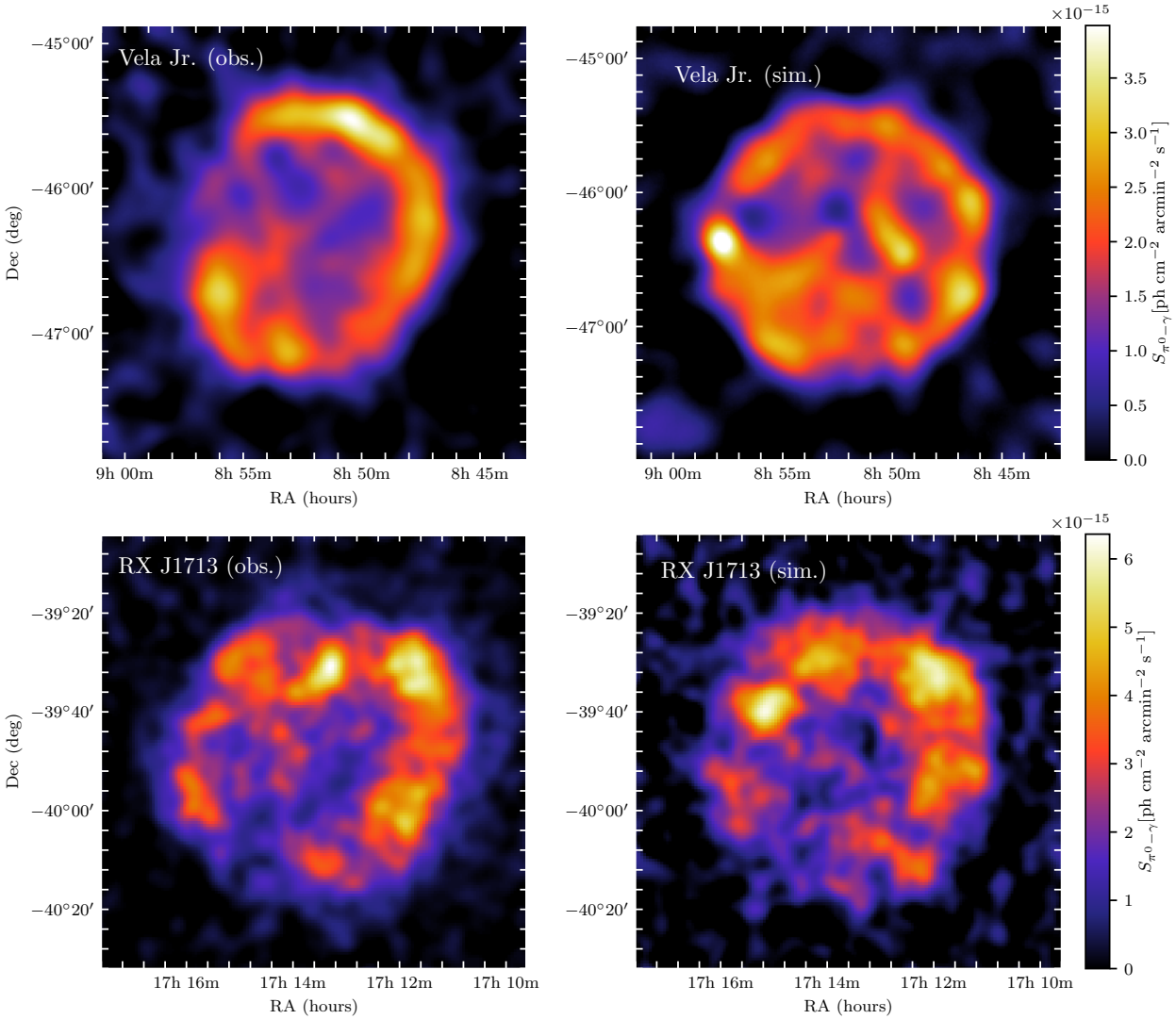

Pais & CP (2020)

RXJ 1713: impact of molecular clumps on TeV γ rays

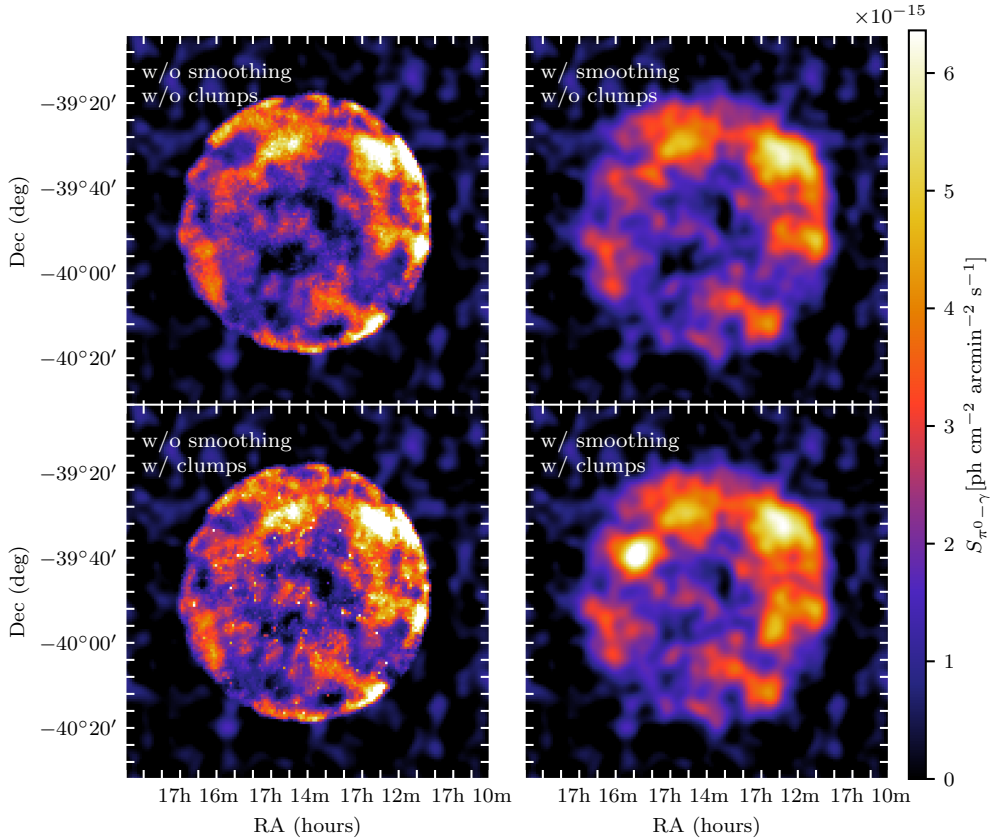

Pais, CP+ (2020)

RXJ 1713: impact of molecular clumps on TeV γ rays

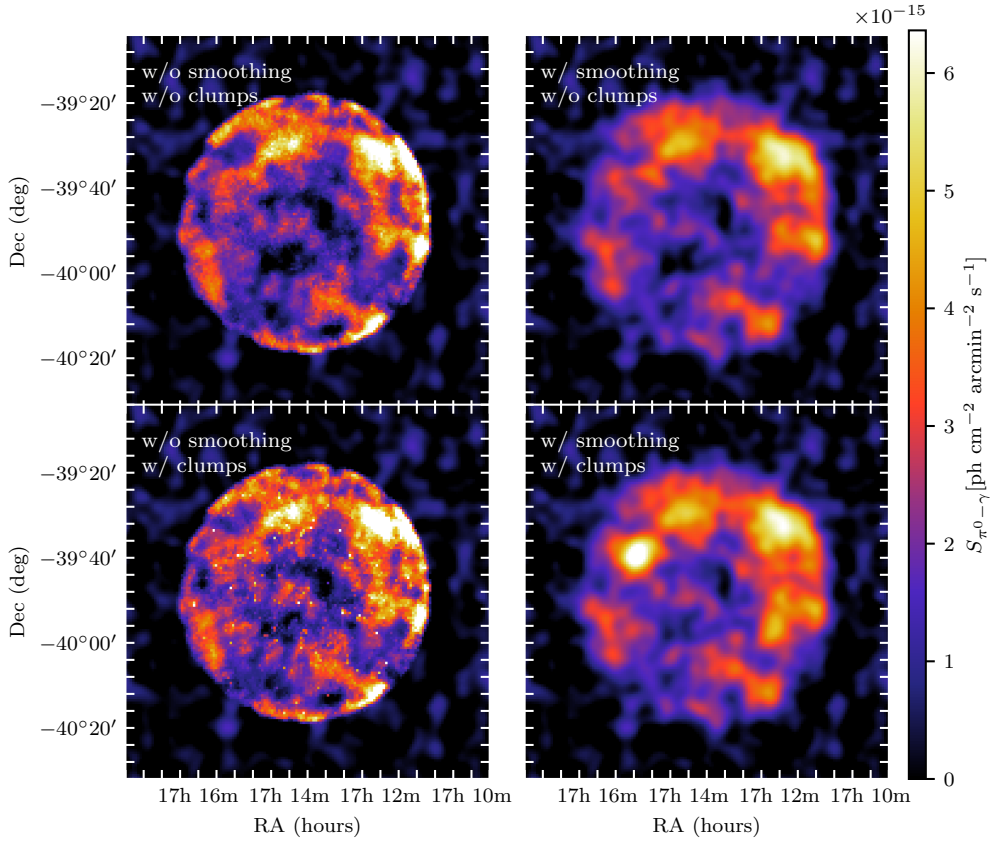

Pais, CP+ (2020)

$\Rightarrow$ clumps can locally dominate γ-ray emission

$\Rightarrow$ large-scale γ-ray morphology traces obliquity-dependent acceleration and magnetic topology

AIP

Straw-man's model: isotropic acceleration and $\delta\rho$

Density inhomogeneities $\delta\rho$ cause patchy TeV maps but a corrugated shock surface

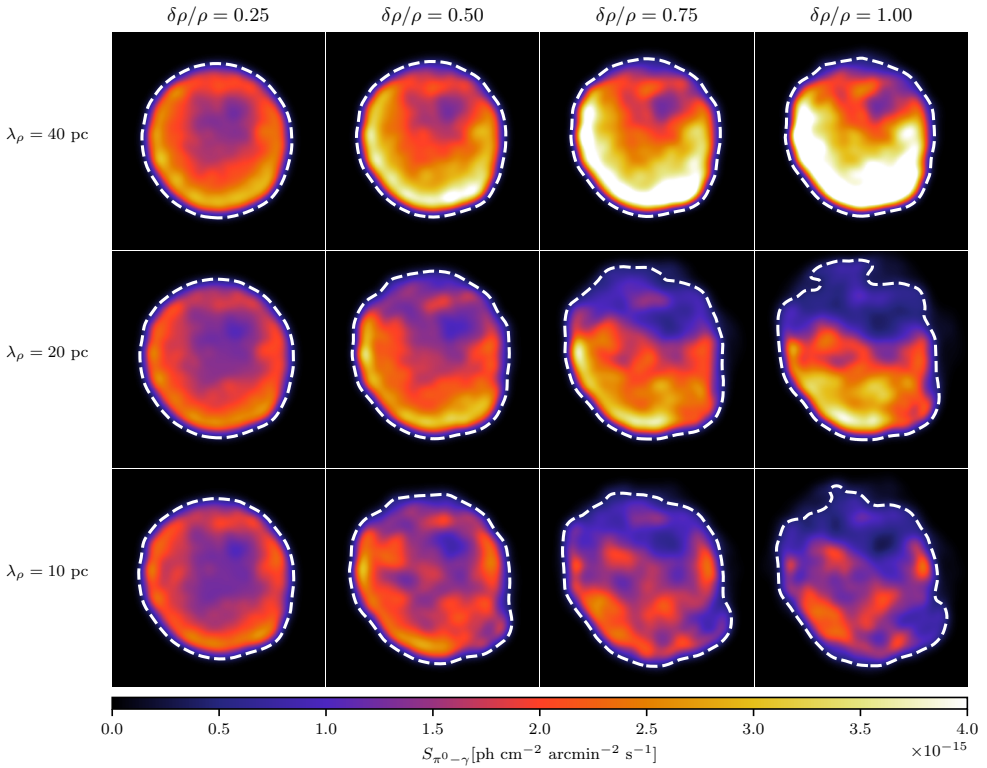

Pais, CP+ (2020)

Straw-man's model: isotropic acceleration and $\delta\rho$

Density inhomogeneities $\delta\rho$ cause patchy TeV maps but a corrugated shock surface

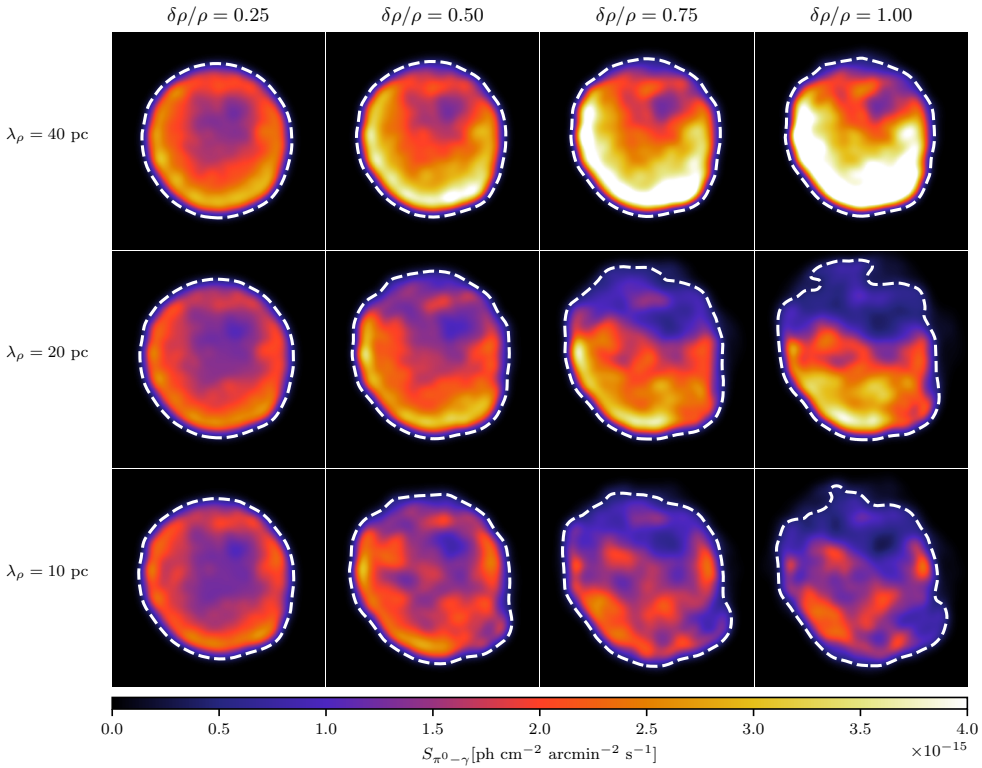

Pais, CP+ (2020)

$\Rightarrow$ anisotropy of corrugated shock surfaces limits (large-scale) density fluctuations $\delta\rho/\rho \lesssim 0.75$

$\Rightarrow$ only obliquity-dep. acceleration explains patchy TeV γ-ray emission

TeV γ rays from shell-type supernova remnants

Varying magnetic coherence scale in simulations of SN 1006 and Vela Junior

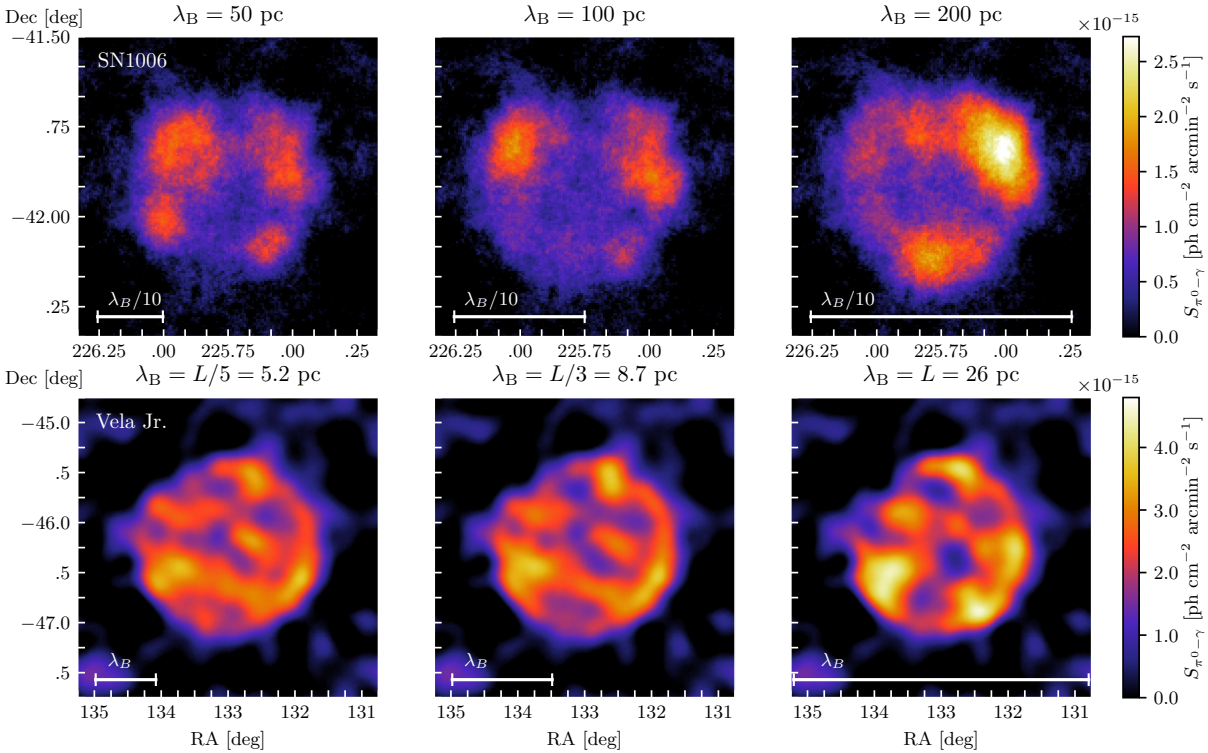

TeV γ rays from shell-type supernova remnants

Varying magnetic coherence scale in simulations of SN 1006 and Vela Junior

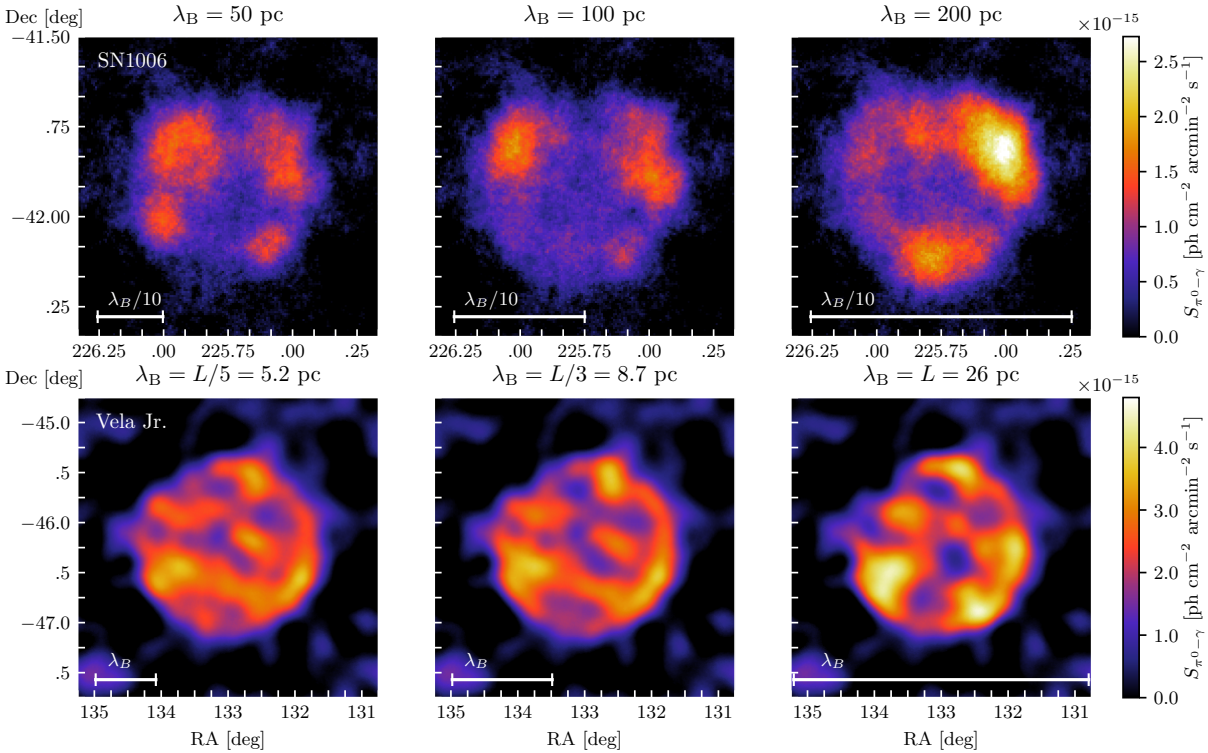

Pais, CP+ (2020)

$\Rightarrow$ Correlation structure of patchy TeV γ-rays constrains magnetic coherence scale in ISM:

SN 1006: $\lambda_B > 200^{+80}_{-10}$ pc Vela Junior: $\lambda_B = 13^{+13}_{-4.3}$ pc

CR electron acceleration: quasi-parallel shocks

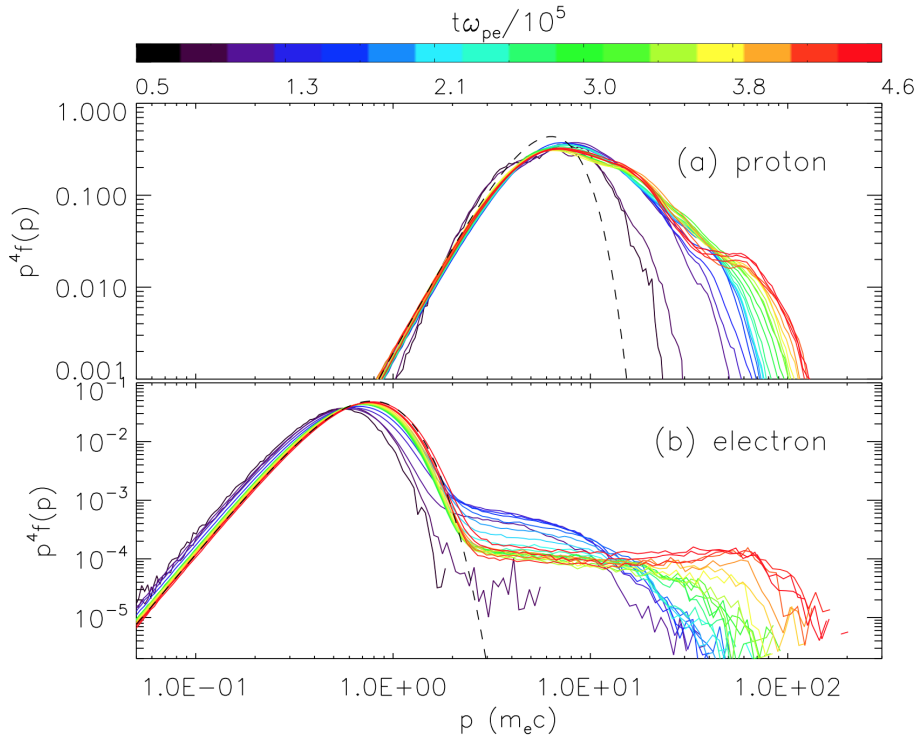

Park, Caprioli, Spitkovsky (2015)

- 1D PIC simulation: simultaneous e^- and p^+ acceleration
- run time $t = 4.6 \times 10^5\, \omega_p^{-1} \approx 8\ \mathrm{s} \left(\frac{n_e}{1\ \mathrm{cm}^{-3}}\right)^{-1/2}$
- quasi-parallel shock (30°): $\varepsilon_{CRe}/\varepsilon_{diss} \lesssim 10^{-3}$

CR electron acceleration: quasi-perpendicular shocks

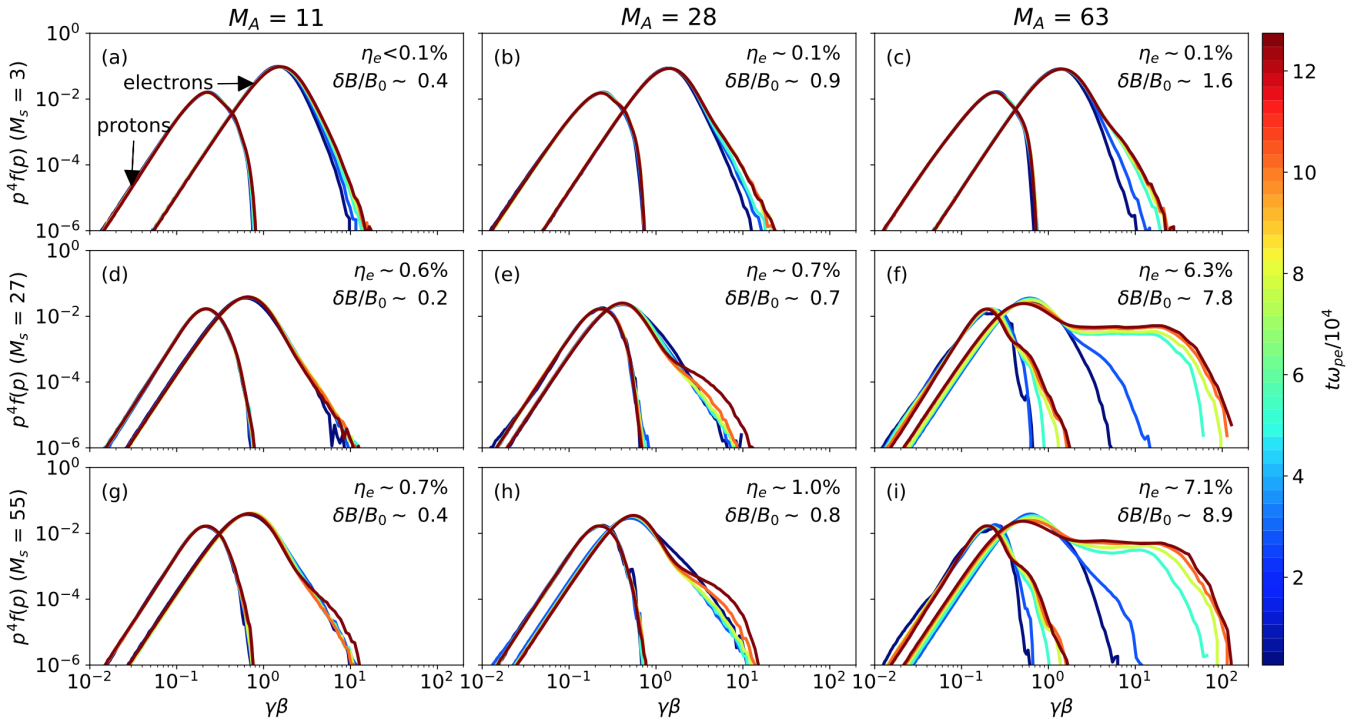

Xu, Spitkovsky, Caprioli (2020), also Riquelme & Spitkovsky (2011), Bohdan+ (2017, 2019, 2020)

- 1D PIC simulation: e^- acceleration, vary $\mathcal{M}_s$ and $\mathcal{M}_A$
- run time $t = 1.2 \times 10^5\, \omega_p^{-1} \approx 2\ \mathrm{s} \left(\frac{n_e}{1\ \mathrm{cm}^{-3}}\right)^{-1/2}$
- quasi-perpendicular shocks (63°): $\varepsilon_{CRe}/\varepsilon_{diss} \approx 10^{-2}$

CREST - Cosmic Ray Electron Spectra evolved in Time

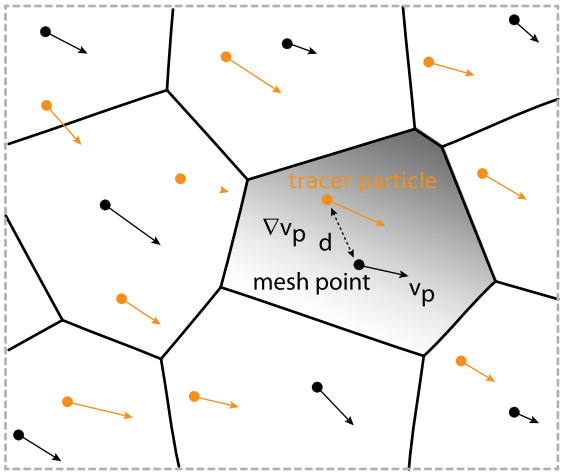

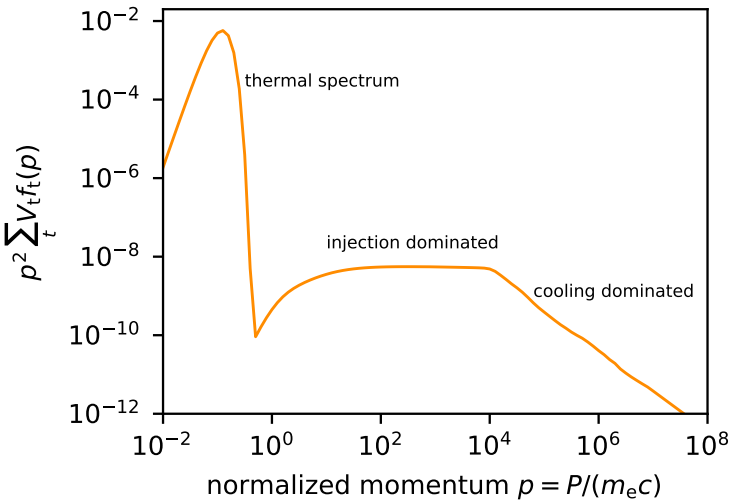

CREST code (Winner, CP+ 2019)

- post-processing MHD simulations
- on Lagrangian particles
  - adiabatic processes
  - Coulomb and radiative losses
  - Fermi-I (re-)acceleration
  - Fermi-II reacceleration
  - secondary electrons

Link to observations

- radio synchrotron
- inverse Compton (IC) γ-ray

Sedov–Taylor blast wave: spectral evolution

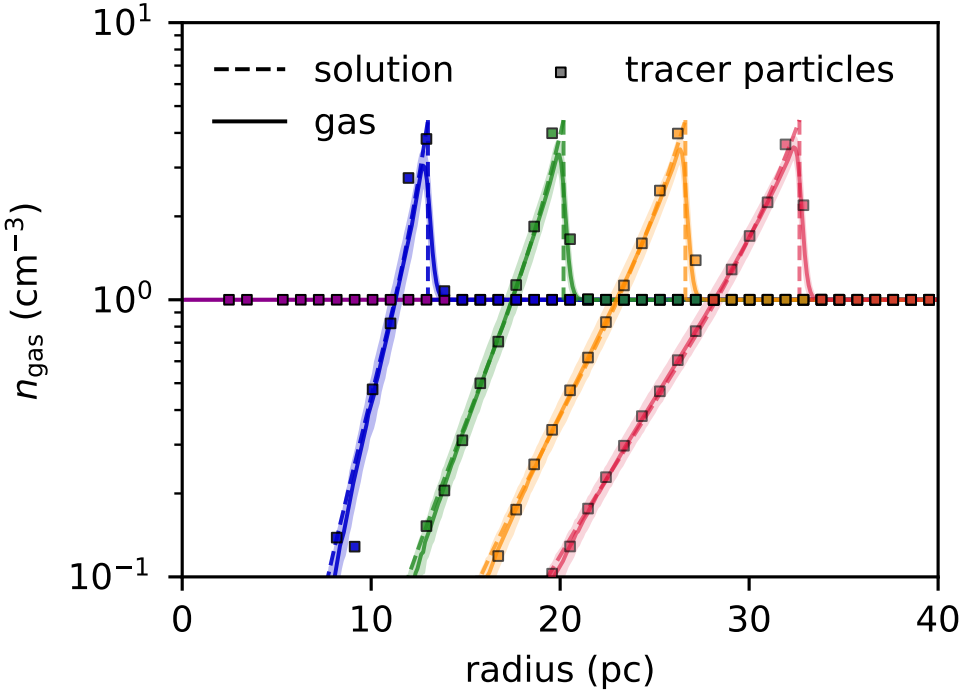

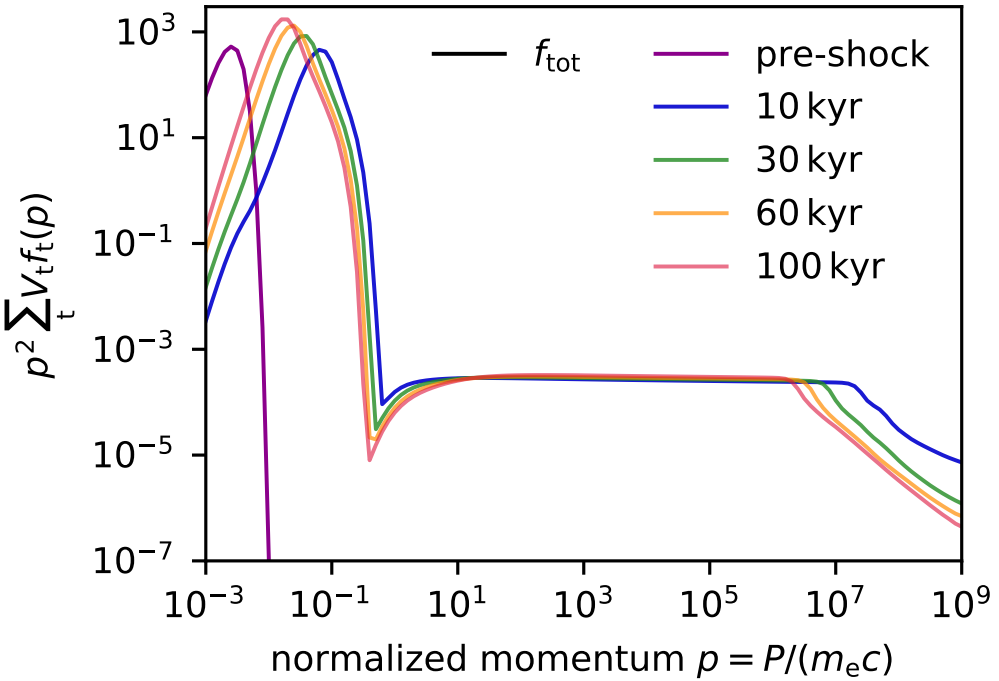

Winner, CP+ (2019)

$E_0 = 10^{51}\,\mathrm{erg},\ n_{\mathrm{gas}} = 1\,\mathrm{cm}^{-3},\ T_0 = 10^4\,\mathrm{K},\ B = 1\,\mu\mathrm{G}$

Sedov–Taylor blast wave: radial contribution

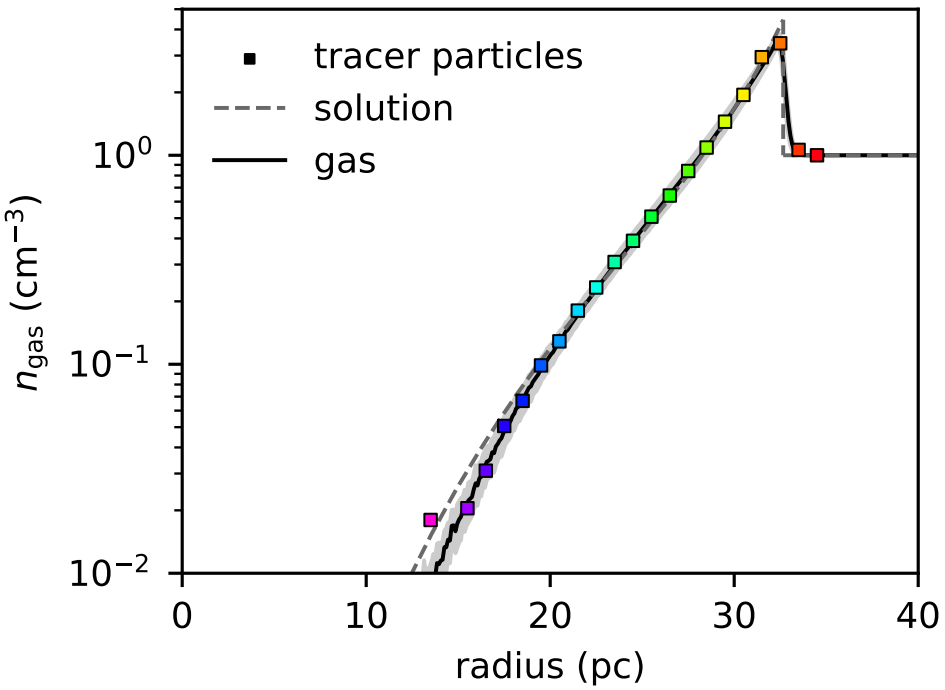

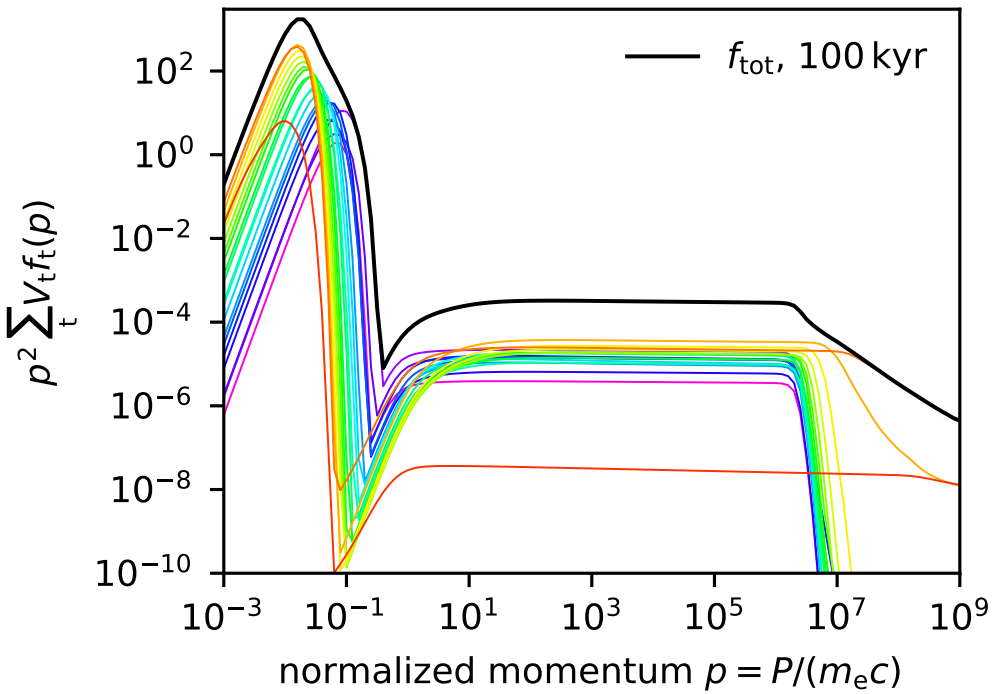

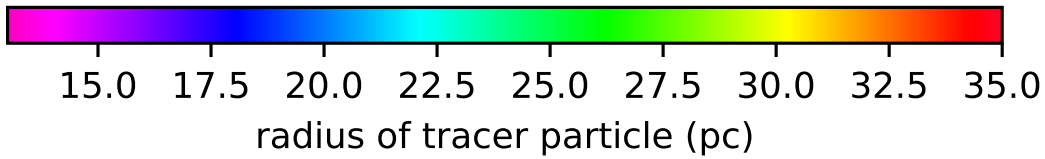

Winner, CP+ (2019)

SN 1006: CR electron acceleration models

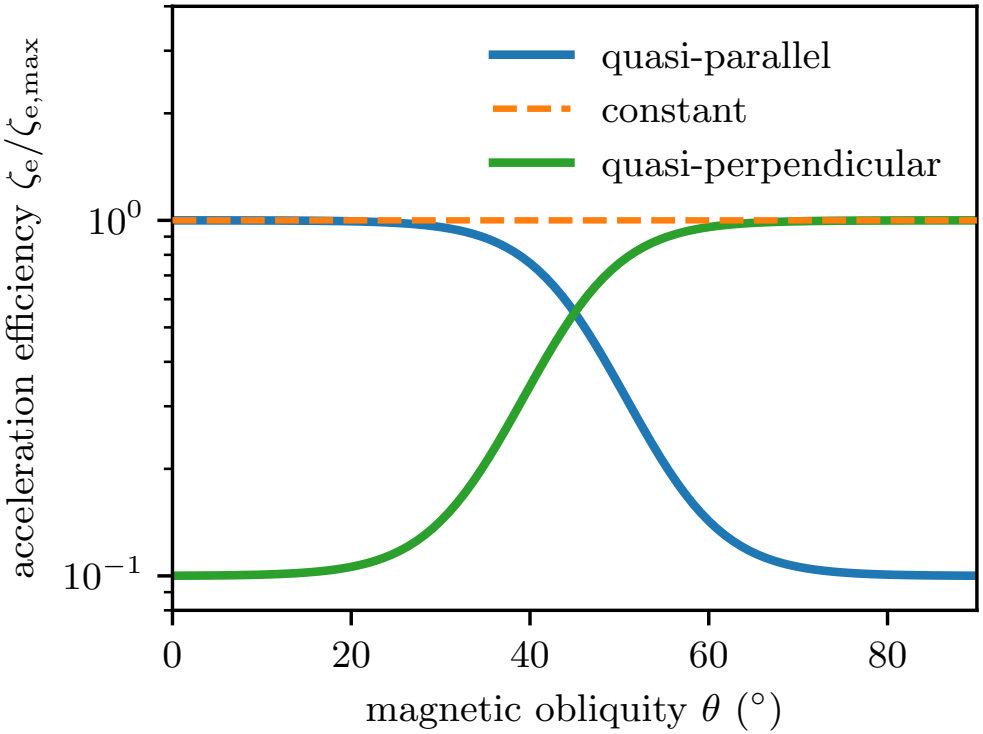

Winner, CP+ (2020)

- different obliquity dependent electron acceleration efficiencies:
  1. preferred quasi-perpendicular acceleration
  2. constant acceleration efficiency
  3. preferred quasi-parallel acceleration

CR electron acceleration: quasi-perpendicular shocks

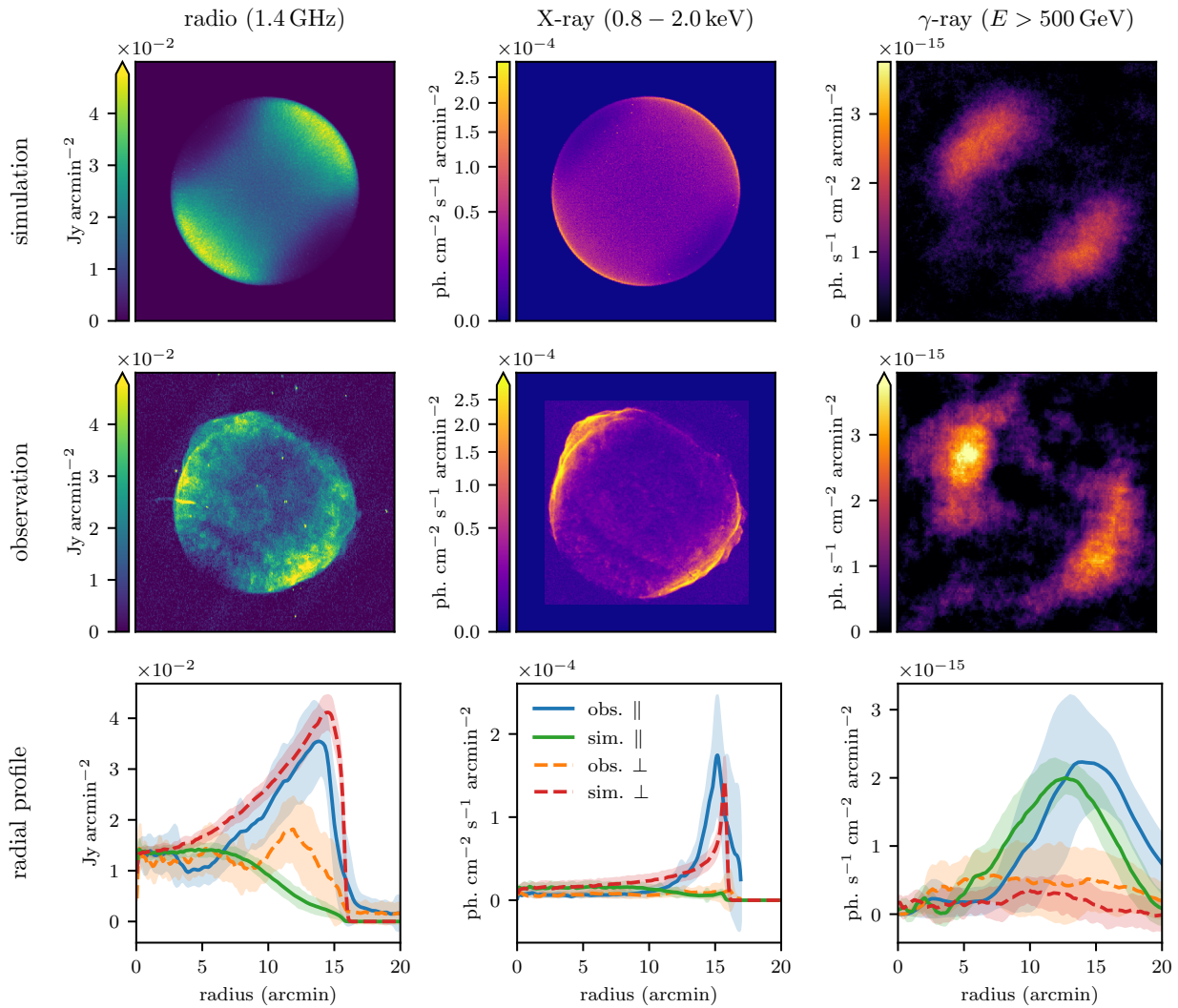

Winner, CP+ (2020)

CR electron acceleration: constant efficiency

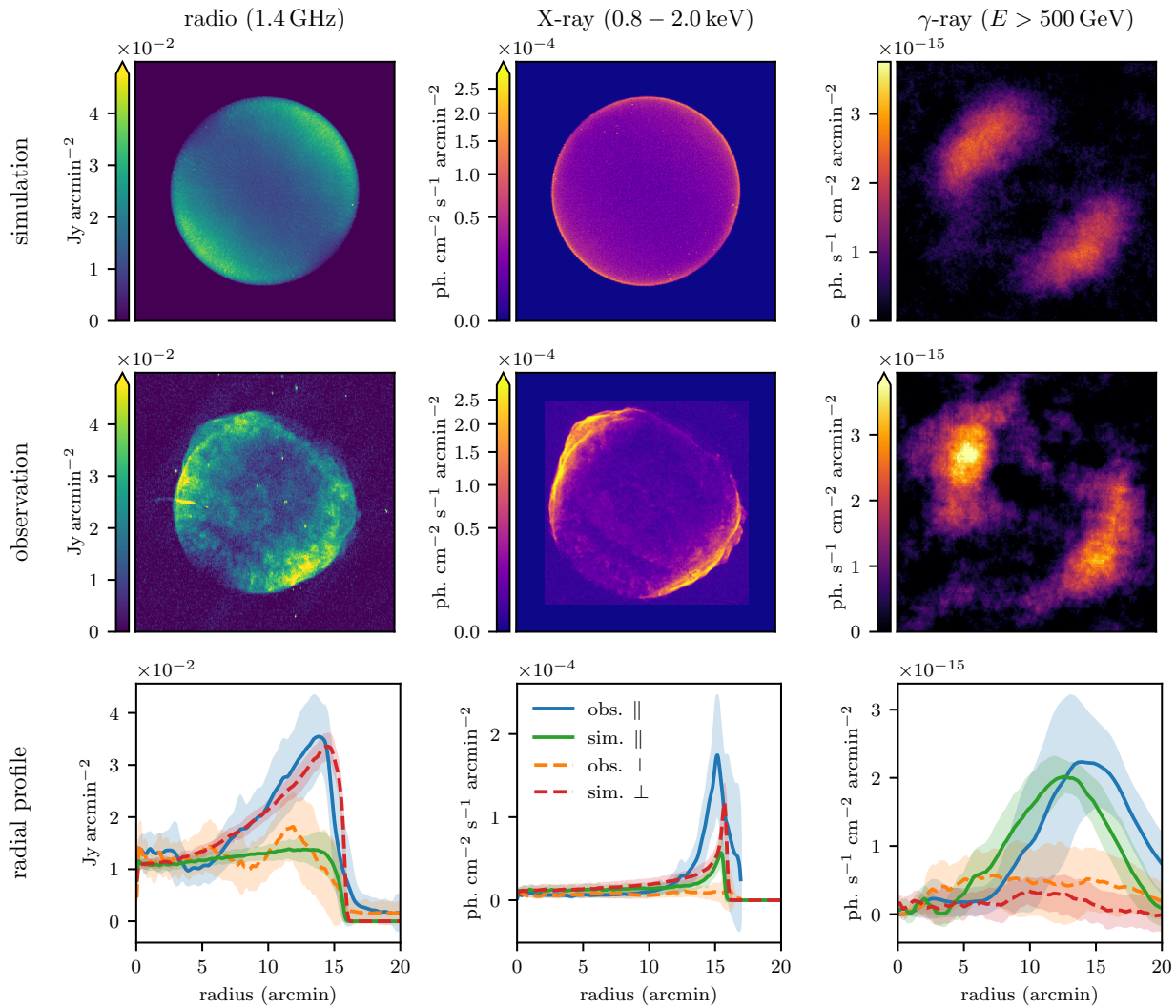

Winner, CP+ (2020)

CR electron acceleration: quasi-parallel shocks

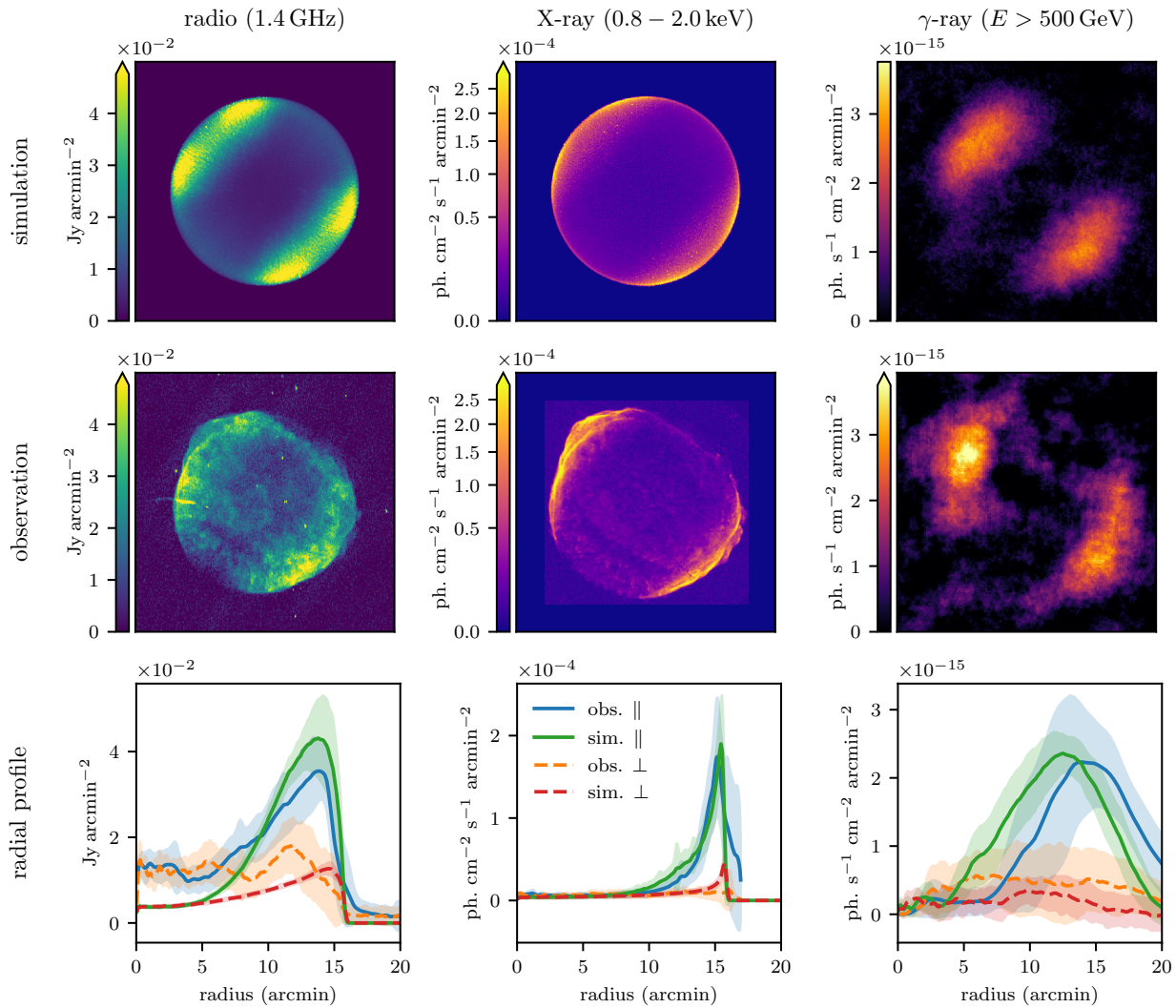

Winner, CP+ (2020)

SN 1006: multi-frequency spectrum

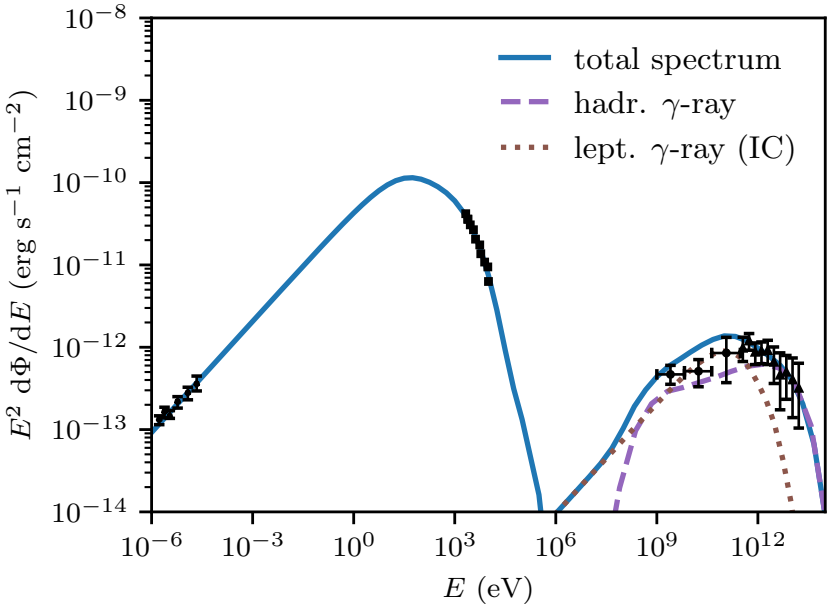

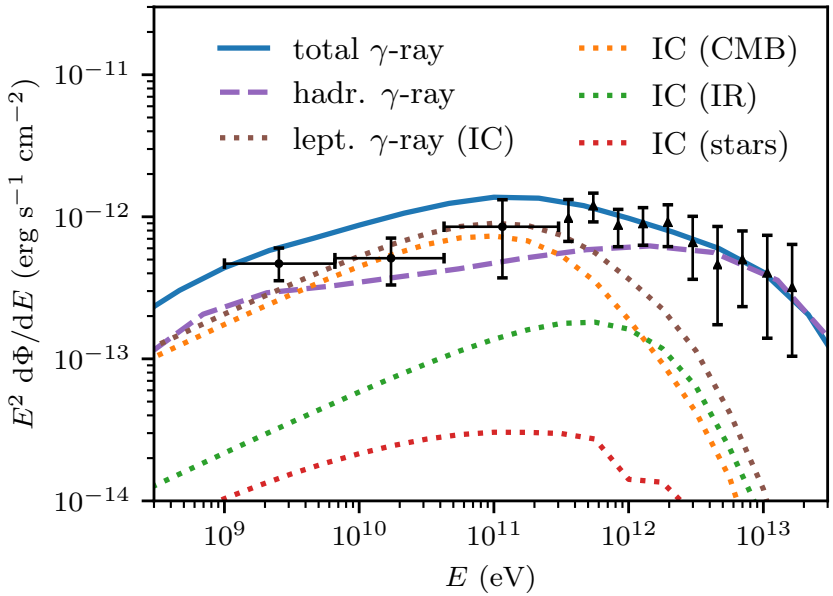

Winner, CP+ (2020)

- quasi-parallel acceleration model fits multi-frequency spectrum

SN 1006: multi-frequency spectrum

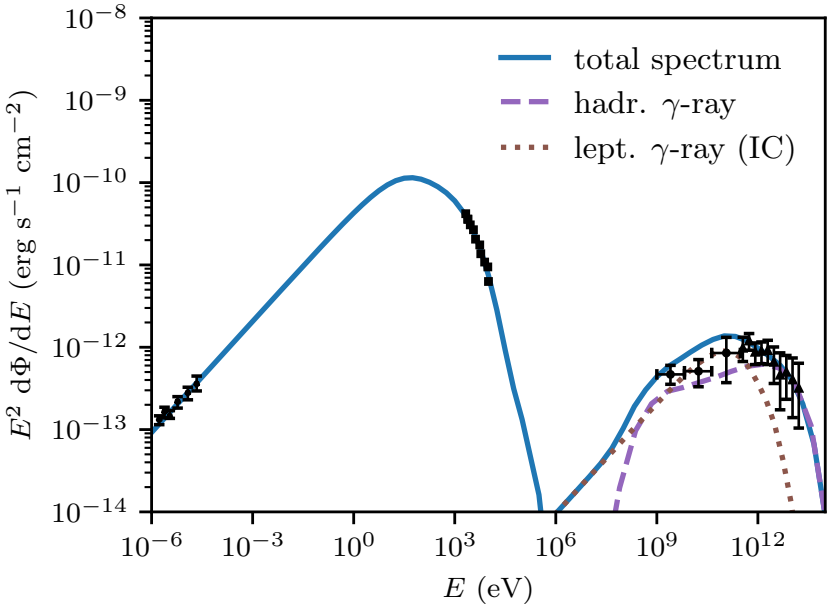

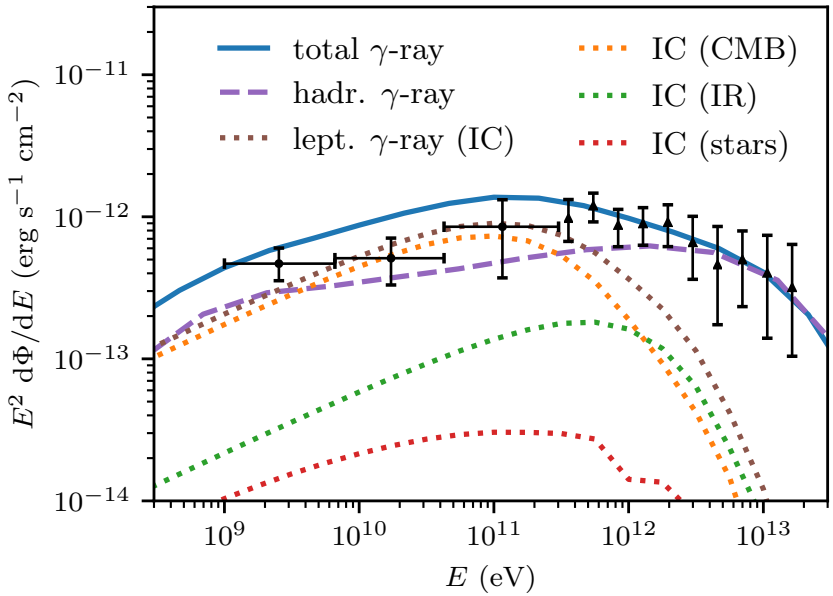

Winner, CP+ (2020)

- quasi-parallel acceleration model fits multi-frequency spectrum
- GeV regime: leptonic inverse Compton dominates
- TeV regime: hadronic pion decay

SN 1006: maps of γ-ray components at $E > 500$ GeV

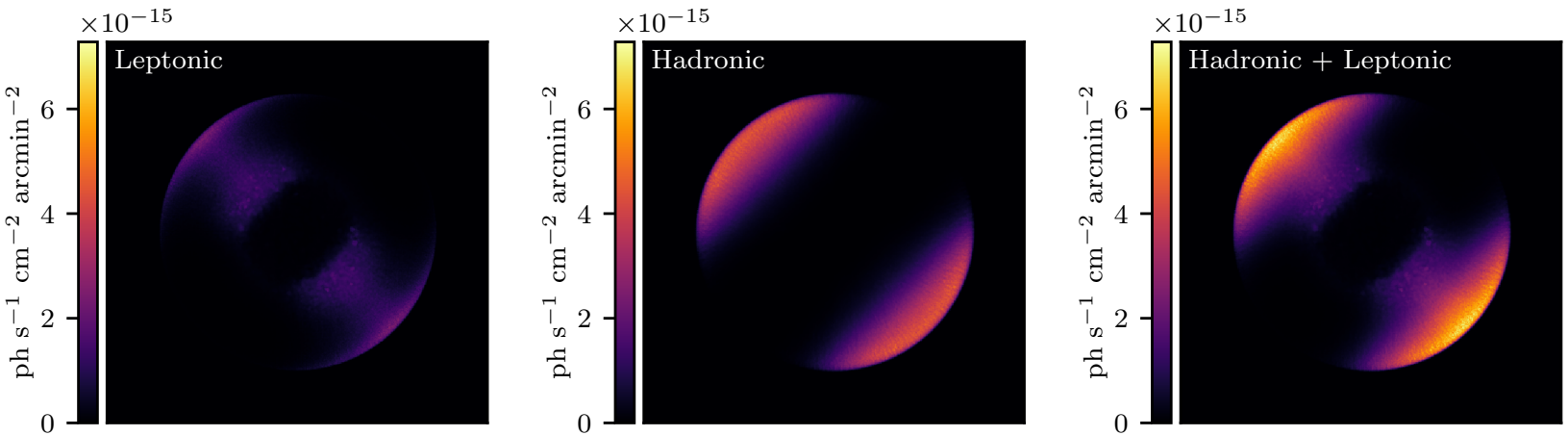

Winner, CP+ (2020)

- hadronic pion decay emission dominant at shock rim
- leptonic IC emission has contributions from SNR interior

SN 1006: magnetic field amplification models

Magnetic amplification due to a turbulent dynamo and Bell's instability

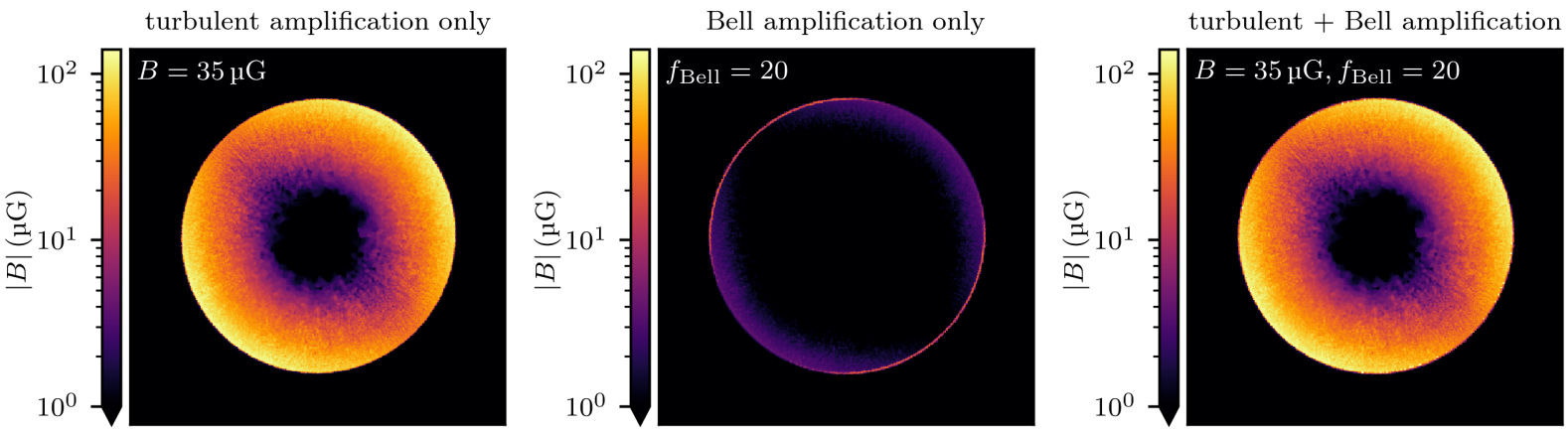

Winner, CP+ (2020)

- magnetic field strength in a slice through the simulated SNRs

SN 1006: magnetic field amplification models

Magnetic amplification due to a turbulent dynamo and Bell's instability

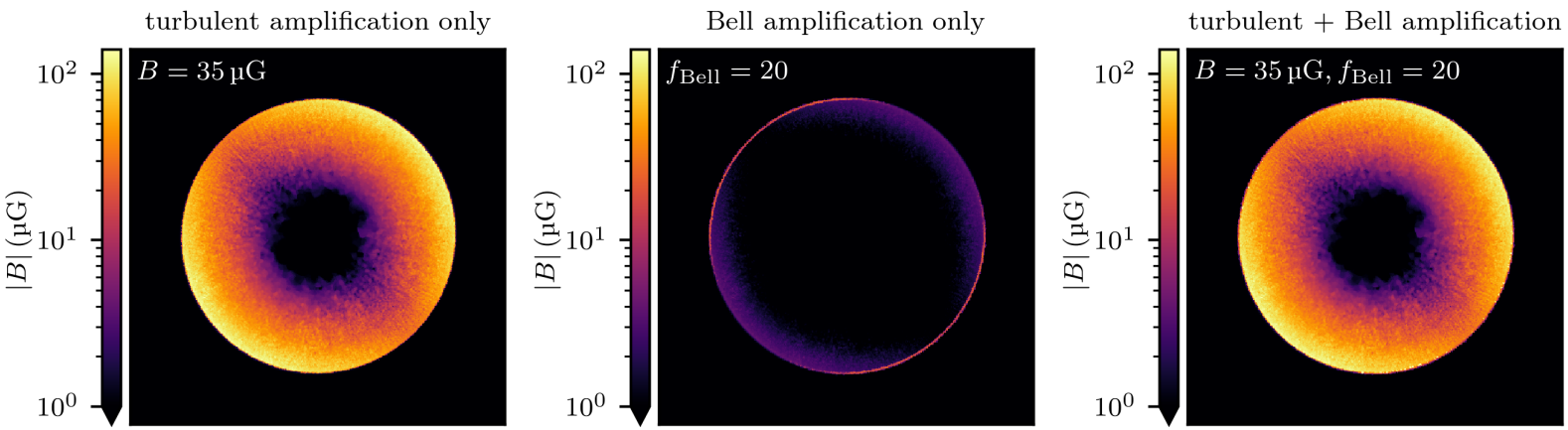

Winner, CP+ (2020)

- magnetic field strength in a slice through the simulated SNRs
- left: effect of turbulent amplification only, maximum realized at quasi-perpendicular shock, adiabatic cooling inside the SNR
- middle: effect of Bell amplification only, f_{Bell} follows obliquity dependence of CR proton efficiency
- right: sum of both, turbulent and Bell amplification

Constraining the volume-filling, turbulent *B* field

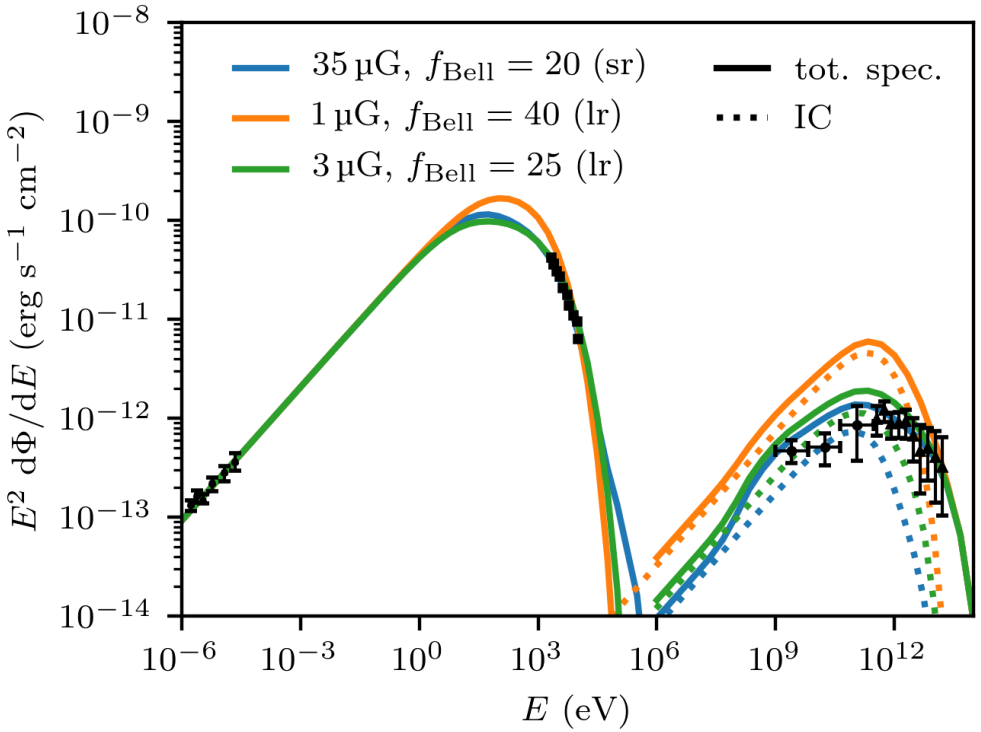

Winner, CP+ (2020)

- multi-frequency spectra: synchrotron (radio + X-rays) and IC and hadronic γ-ray emission

Constraining the volume-filling, turbulent ***B*** field

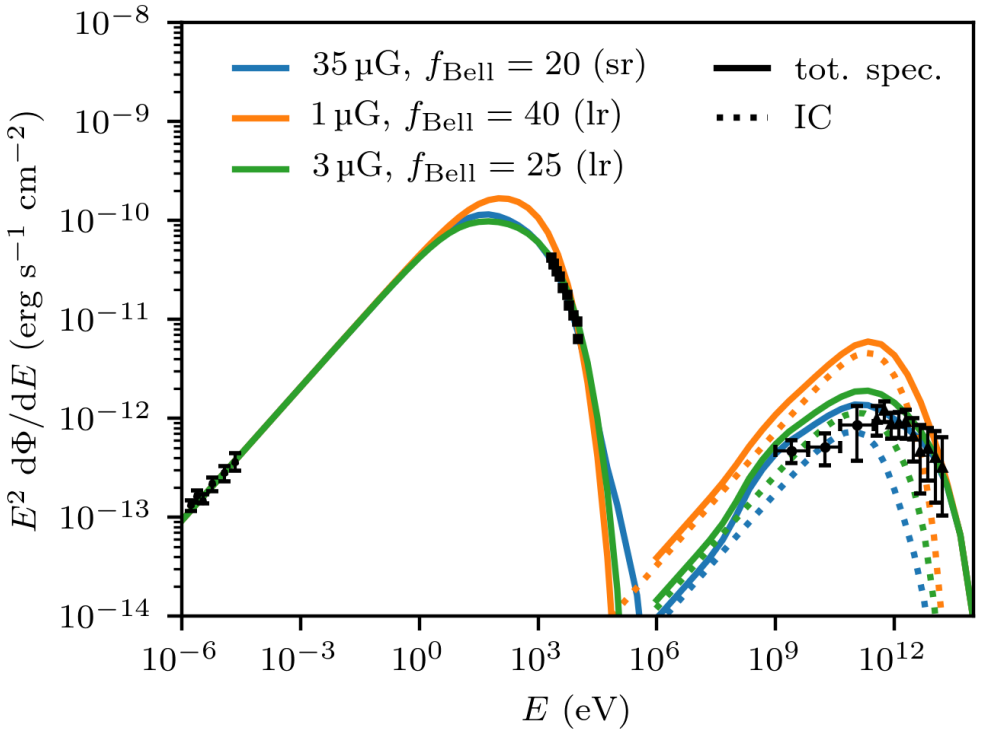

Winner, CP+ (2020)

- multi-frequency spectra: synchrotron (radio + X-rays) and IC and hadronic γ-ray emission
- strong, volume-filling ***B*** field (≈ 35 μG) required to suppress IC γ-ray component and to match steep X-ray spectrum

Constraining the damping of Bell-amplified *B* field

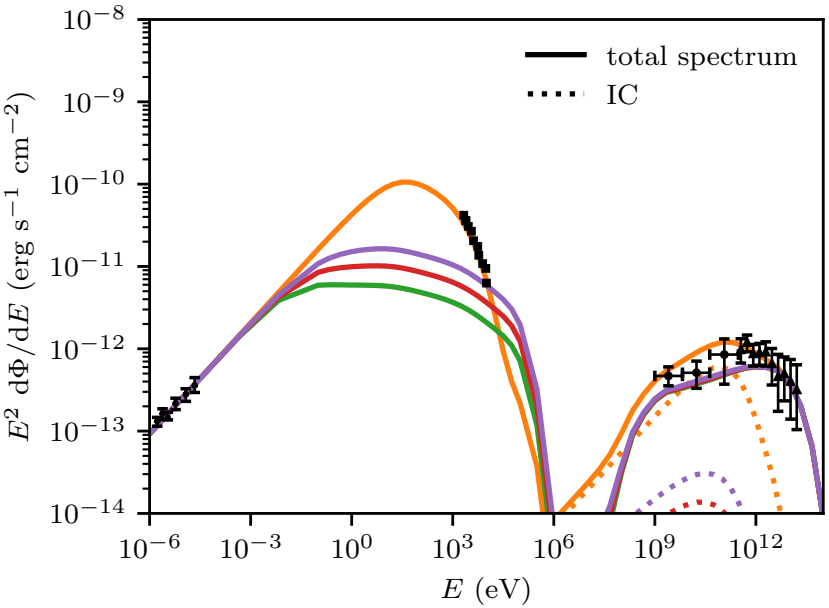

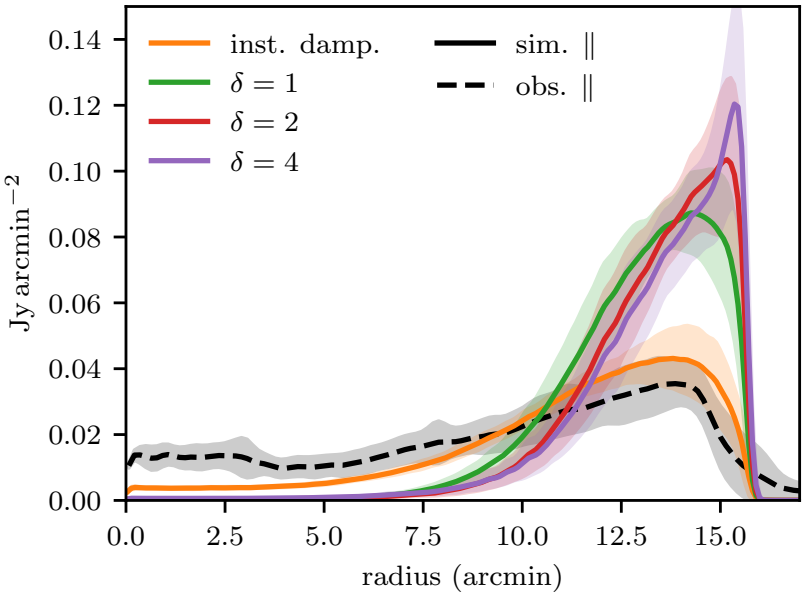

Winner, CP+ (2020)

- multi-frequency spectra (left) and radial radio profiles (right) for different decay models of the Bell-amplified ***B*** field: $B \propto n^{\delta} B_{\mathrm{amp}}$

Constraining the damping of Bell-amplified $\boldsymbol{B}$ field

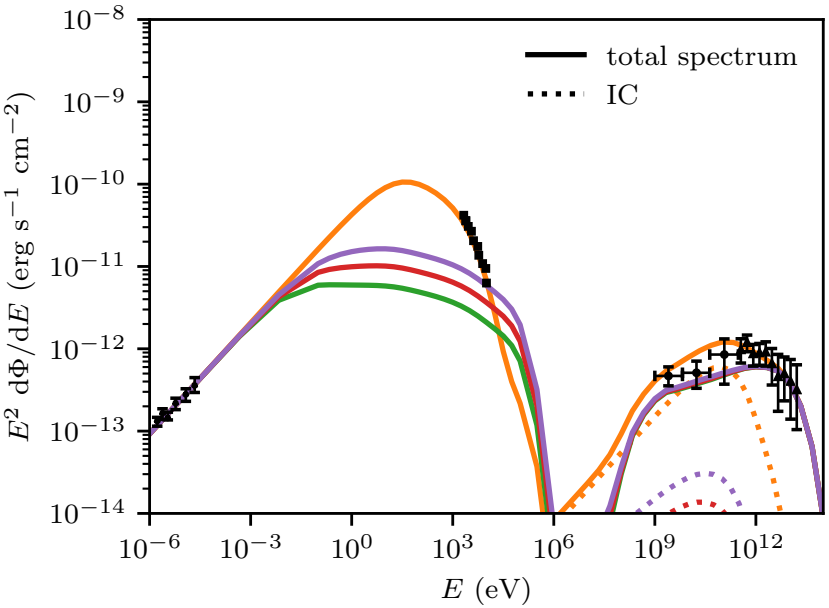

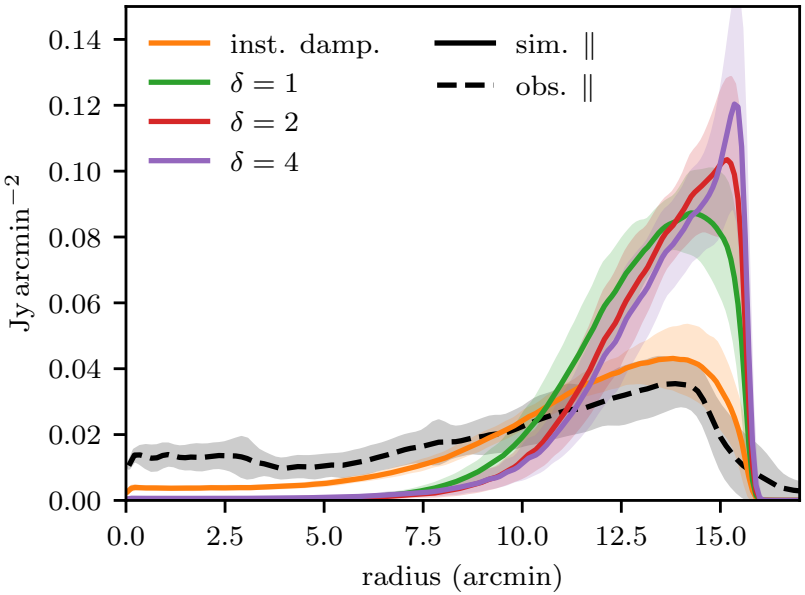

Winner, CP+ (2020)

- multi-frequency spectra (left) and radial radio profiles (right) for different decay models of the Bell-amplified $\boldsymbol{B}$ field: $B \propto n^{\delta} B_{\mathrm{amp}}$
- smooth radio profile and steep X-ray spectrum requires slow CRe cooling and fast damping of Bell modes ($\sim$ 100 gyroradii for TeV particles)

SN 1006: best-fit multi-frequency spectrum

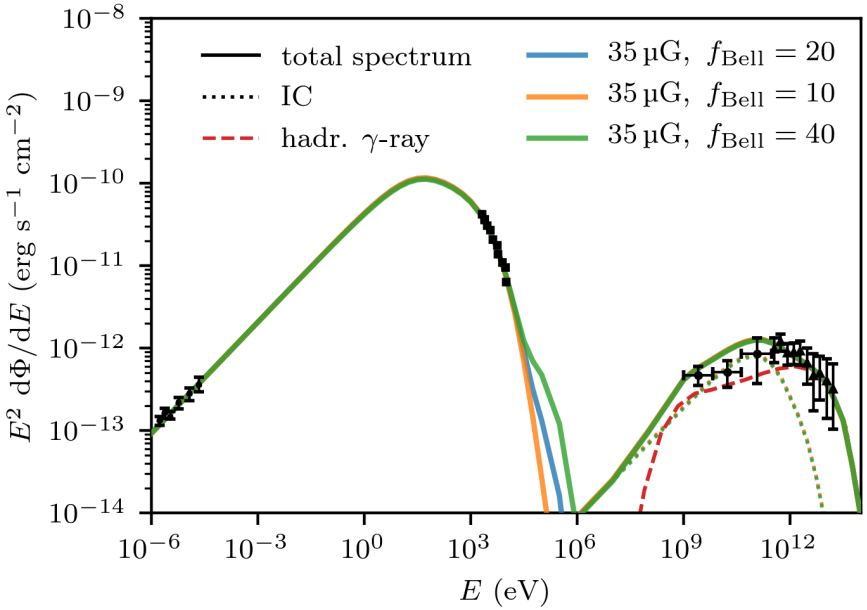

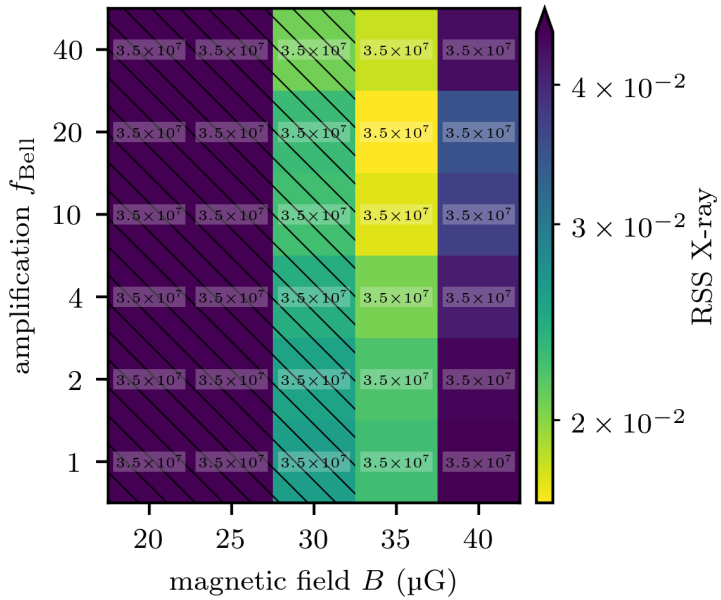

Winner, CP+ (2020)

- parameter optimization of magnetic amplification processes
- strong ($\approx$ 35 μG) volume-filling ***B*** field (turbulent dynamo): lower *B* field excluded by IC component
- Bell-amplification factor $f_{\rm Bell}$ 10 – 20 weakly constrained

Outline

Cosmic ray transport: an extreme multi-scale problem

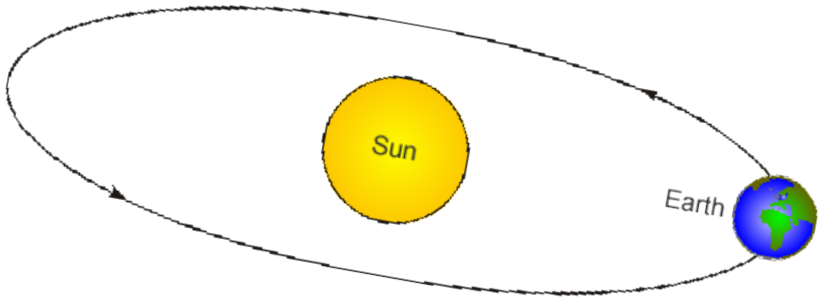

Milky Way-like galaxy:

$$r_{\rm gal} \sim 10^4 \text{ pc}$$

gyro-orbit of GeV cosmic ray:

$$r_{\rm cr} = \frac{p_\perp}{e\,B_{\mu\rm G}} \sim 10^{-6} \text{ pc} \sim \frac{1}{4} \text{ AU}$$

$\Rightarrow$ need to develop a **fluid theory for a collisionless, non-Maxwellian component!**

Zweibel (2017), Jiang & Oh (2018), Thomas & CP (2019)

AIP

Interactions of CRs and magnetic fields

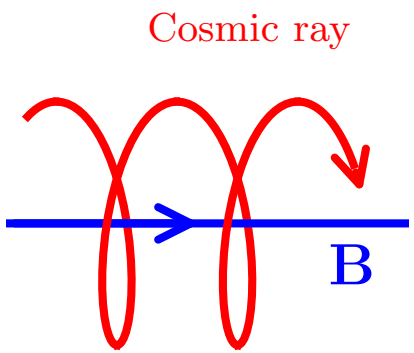

sketch: Jacob

Interactions of CRs and magnetic fields

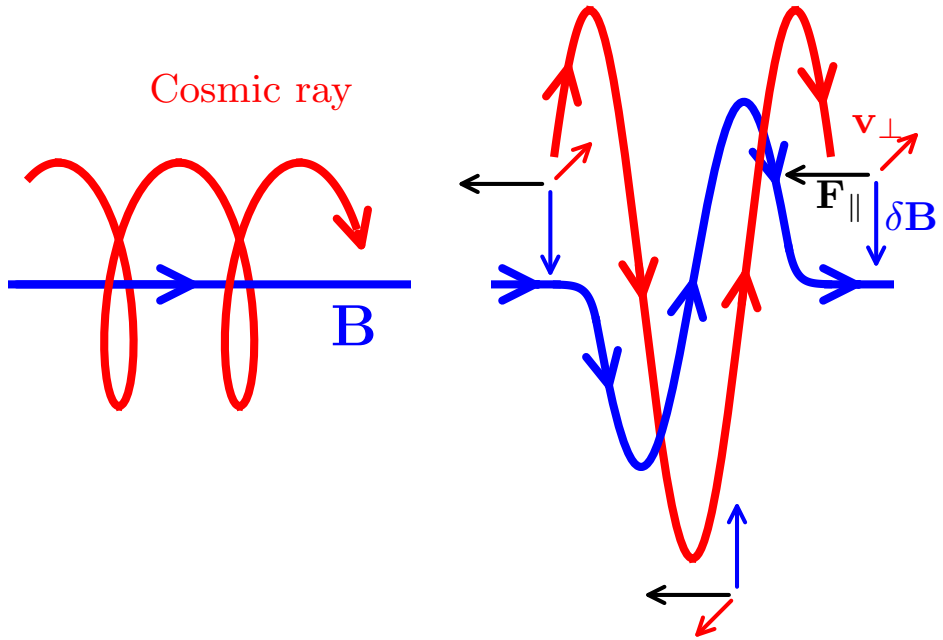

sketch: Jacob

- **gyro resonance:** $\omega - k_\parallel v_\parallel = n\Omega$

  Doppler-shifted MHD frequency is a multiple of the CR gyrofrequency

Interactions of CRs and magnetic fields

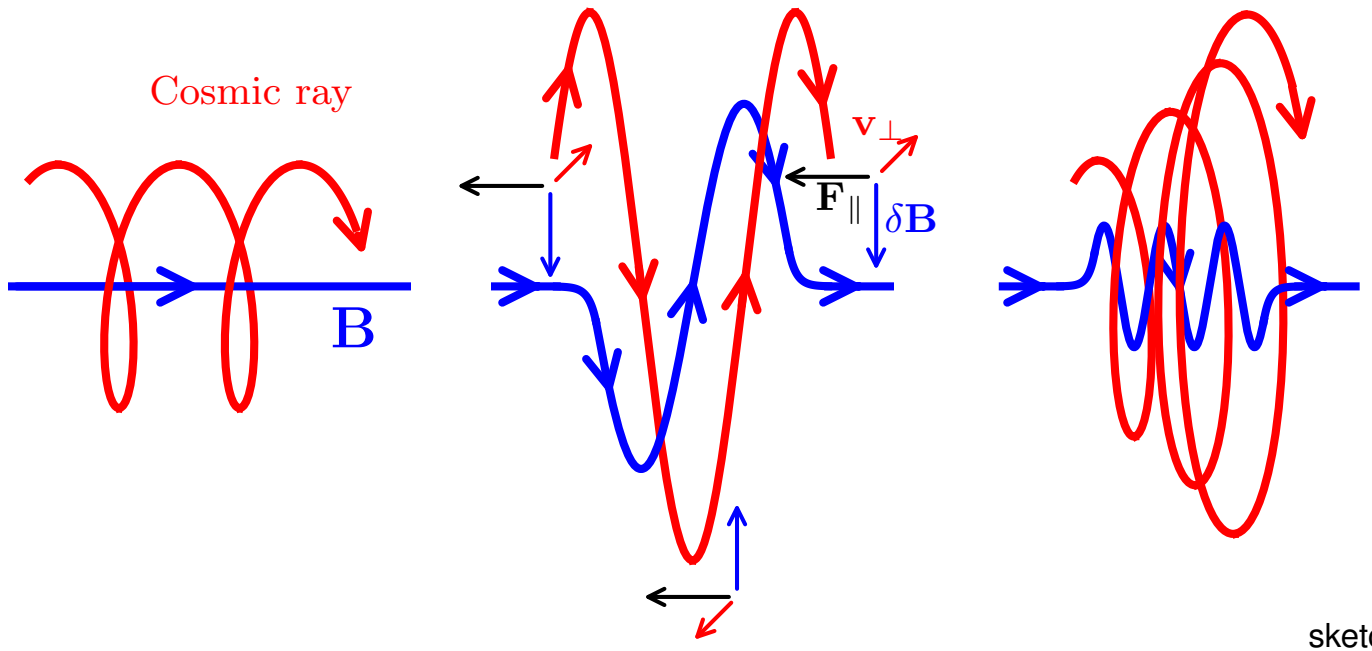

sketch: Jacob

- **gyro resonance:** $\omega - k_\parallel v_\parallel = n\Omega$

  Doppler-shifted MHD frequency is a multiple of the CR gyrofrequency
- CRs scatter on magnetic fields $\rightarrow$ isotropization of CR momenta

CR streaming and diffusion

- **CR streaming instability:** Kulsrud & Pearce 1969
  - if $v_{cr} > v_a$, CR flux excites and amplifies an Alfvén wave field in resonance with the gyroradii of CRs
  - scattering off of this wave field limits the (GeV) CRs' bulk speed $\sim v_a$
  - wave damping: transfer of CR energy and momentum to the thermal gas

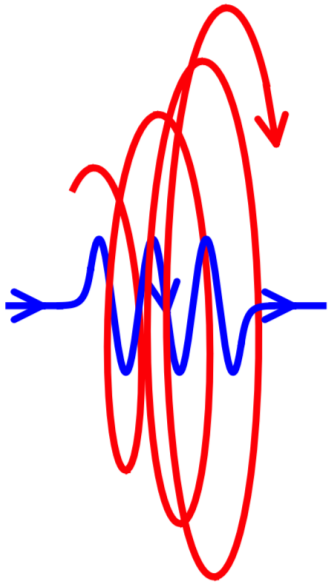

AIP

CR streaming and diffusion

- **CR streaming instability:** Kulsrud & Pearce 1969
  - if $v_{cr} > v_a$, CR flux excites and amplifies an Alfvén wave field in resonance with the gyroradii of CRs
  - scattering off of this wave field limits the (GeV) CRs' bulk speed $\sim v_a$
  - wave damping: transfer of CR energy and momentum to the thermal gas

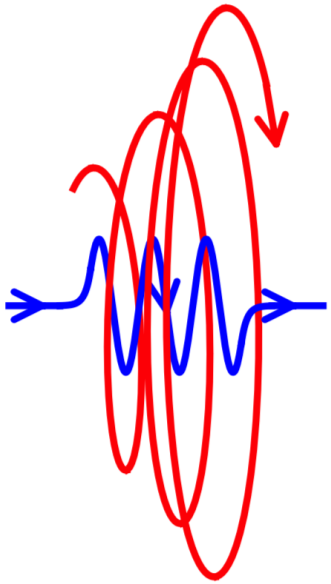

$\rightarrow$ *CRs exert pressure on thermal gas via scattering on Alfvén waves*

CR streaming and diffusion

- **CR streaming instability:** Kulsrud & Pearce 1969
  - if $v_{cr} > v_a$, CR flux excites and amplifies an Alfvén wave field in resonance with the gyroradii of CRs
  - scattering off of this wave field limits the (GeV) CRs' bulk speed $\sim v_a$
  - wave damping: transfer of CR energy and momentum to the thermal gas

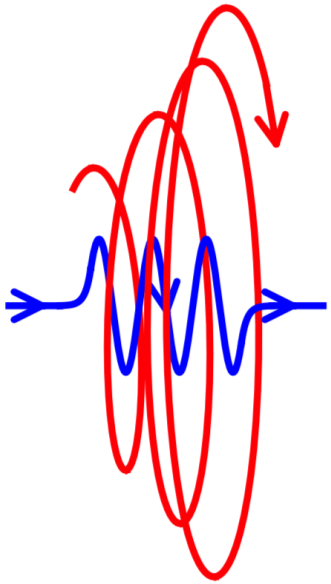

$\rightarrow$ *CRs exert pressure on thermal gas via scattering on Alfvén waves*

weak wave damping: strong coupling $\rightarrow$ CR stream with waves
strong wave damping: less waves to scatter $\rightarrow$ CR diffusion prevails

AIP

Modes of CR propagation

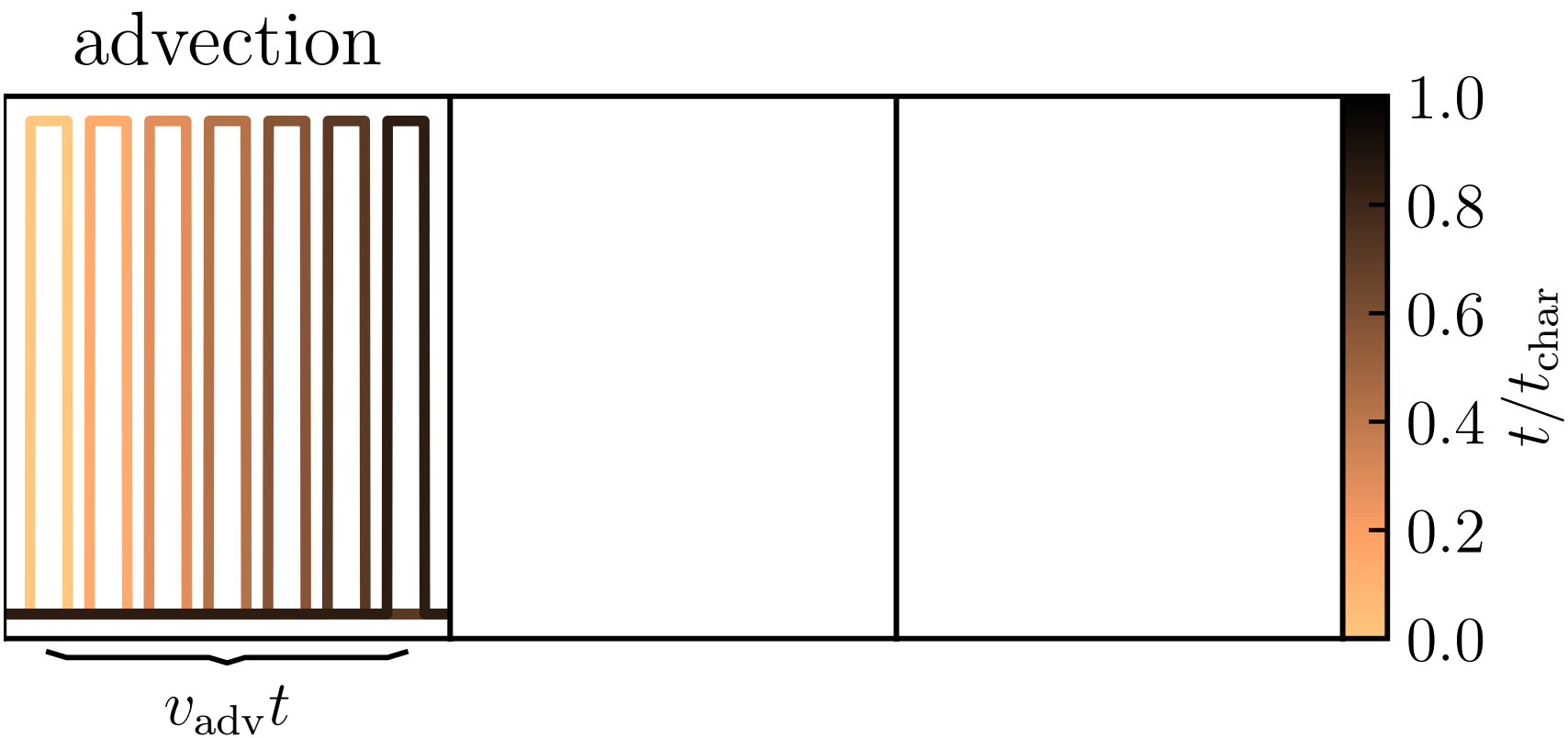

Thomas, CP, Enßlin (2020)

AIP

Modes of CR propagation

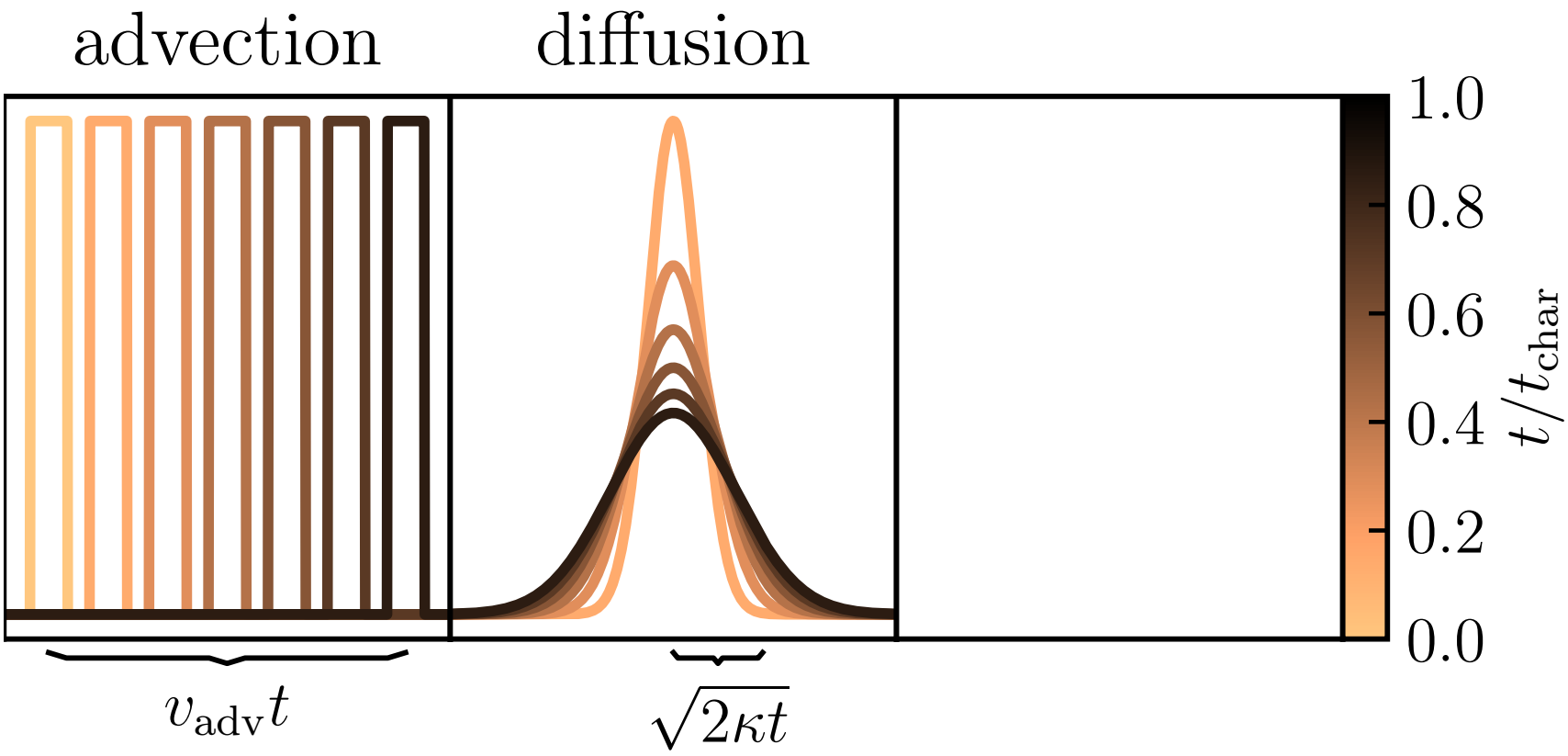

Thomas, CP, Enßlin (2020)

AIP

Modes of CR propagation

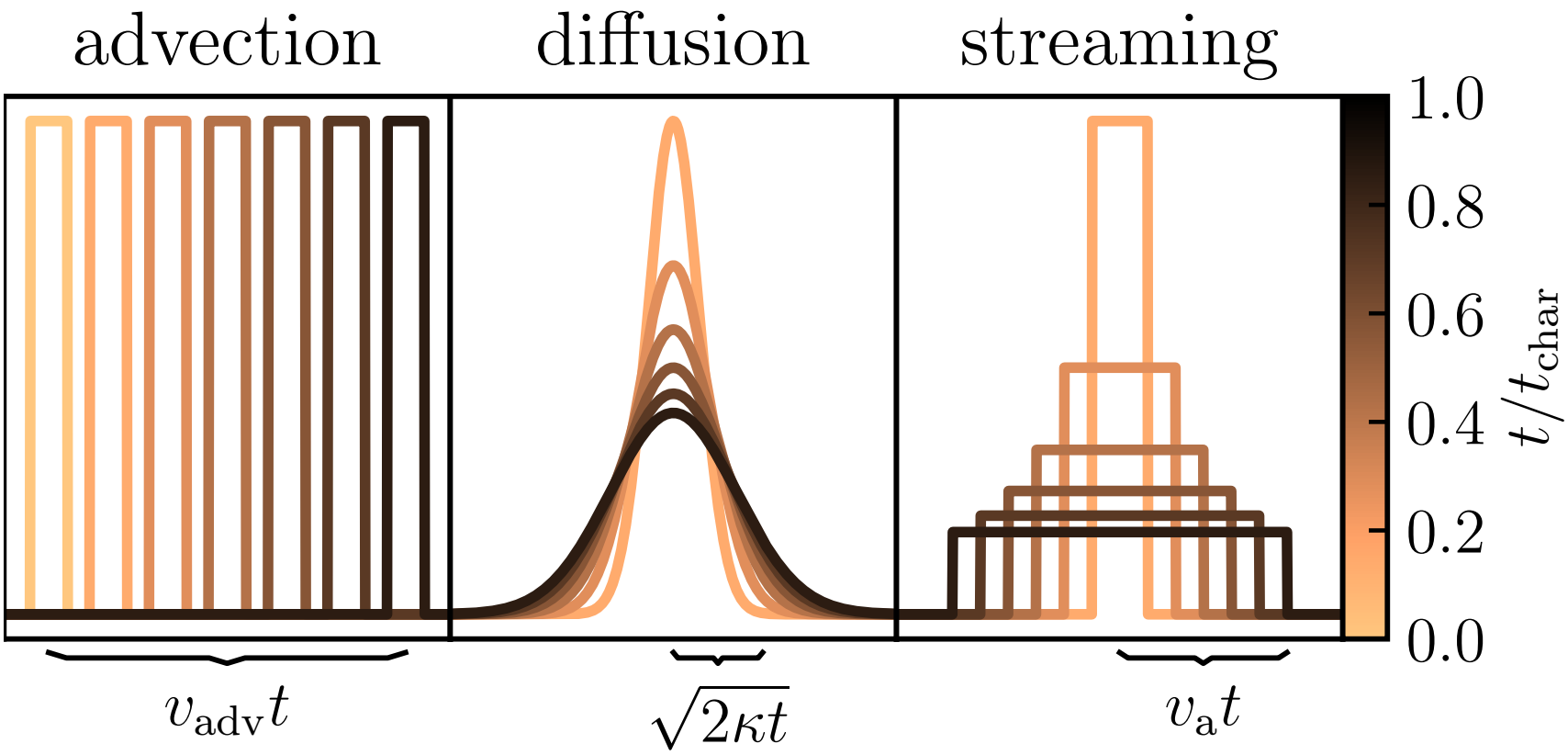

Thomas, CP, Enßlin (2020)

AIP

CR vs. radiation hydrodynamics

- capitalize on analogies of CR and radiation hydrodynamics (Jiang & Oh 2018)
  derive two-moment equations from CR Vlasov equation (Thomas & CP 2019)

CR vs. radiation hydrodynamics

- capitalize on analogies of CR and radiation hydrodynamics (Jiang & Oh 2018) derive two-moment equations from CR Vlasov equation (Thomas & CP 2019)
- lab-frame equ's for CR energy and momentum density, $\varepsilon_{\rm cr}$ and $\boldsymbol{f}_{\rm cr}/c^2$

$$\frac{\partial \varepsilon_{\rm cr}}{\partial t} + \boldsymbol{\nabla}\cdot\boldsymbol{f}_{\rm cr} = -\boldsymbol{w}_\pm \cdot \frac{\boldsymbol{bb}}{3\kappa_\pm}\cdot[\boldsymbol{f}_{\rm cr} - \boldsymbol{w}_\pm(\varepsilon_{\rm cr}+P_{\rm cr})] - \boldsymbol{v}\cdot\boldsymbol{g}_{\rm Lorentz} + S_\varepsilon$$

$$\frac{1}{c^2}\frac{\partial \boldsymbol{f}_{\rm cr}}{\partial t} + \boldsymbol{\nabla}\cdot\mathbf{P}_{\rm cr} = -\frac{\boldsymbol{bb}}{3\kappa_\pm}\cdot[\boldsymbol{f}_{\rm cr} - \boldsymbol{w}_\pm(\varepsilon_{\rm cr}+P_{\rm cr})] - \boldsymbol{g}_{\rm Lorentz} + \boldsymbol{S}_f$$

Alfvén wave velocity in lab frame: $\boldsymbol{w}_\pm = \boldsymbol{v} \pm \boldsymbol{v}_{\rm a}$,
CR scattering frequency $\bar{\nu}_\pm = c^2/(3\kappa_\pm)$

CR vs. radiation hydrodynamics

- capitalize on analogies of CR and radiation hydrodynamics (Jiang & Oh 2018) derive two-moment equations from CR Vlasov equation (Thomas & CP 2019)
- lab-frame equ's for CR energy and momentum density, $\varepsilon_{\rm cr}$ and $\boldsymbol{f}_{\rm cr}/c^2$

$$\frac{\partial \varepsilon_{\rm cr}}{\partial t} + \boldsymbol{\nabla}\cdot\boldsymbol{f}_{\rm cr} = -\boldsymbol{w}_\pm \cdot \frac{\boldsymbol{bb}}{3\kappa_\pm}\cdot[\boldsymbol{f}_{\rm cr} - \boldsymbol{w}_\pm(\varepsilon_{\rm cr}+P_{\rm cr})] - \boldsymbol{v}\cdot\boldsymbol{g}_{\rm Lorentz} + S_\varepsilon$$

$$\frac{1}{c^2}\frac{\partial \boldsymbol{f}_{\rm cr}}{\partial t} + \boldsymbol{\nabla}\cdot\mathbf{P}_{\rm cr} = -\frac{\boldsymbol{bb}}{3\kappa_\pm}\cdot[\boldsymbol{f}_{\rm cr} - \boldsymbol{w}_\pm(\varepsilon_{\rm cr}+P_{\rm cr})] - \boldsymbol{g}_{\rm Lorentz} + \boldsymbol{S}_f$$

Alfvén wave velocity in lab frame: $\boldsymbol{w}_\pm = \boldsymbol{v} \pm \boldsymbol{v}_{\rm a}$,
CR scattering frequency $\bar{\nu}_\pm = c^2/(3\kappa_\pm)$

- lab-frame equ's for radiation energy and momentum density, ε and $\boldsymbol{f}/c^2$

(Mihalas & Mihalas, 1984, Lowrie+ 1999):

$$\frac{\partial \varepsilon}{\partial t} + \boldsymbol{\nabla}\cdot\boldsymbol{f} = -\sigma_{\rm s}\boldsymbol{v}\cdot[\boldsymbol{f} - \boldsymbol{v}\cdot(\varepsilon\mathbf{1}+\mathbf{P})] + S_{\rm a}$$

$$\frac{1}{c^2}\frac{\partial \boldsymbol{f}}{\partial t} + \boldsymbol{\nabla}\cdot\mathbf{P} = -\sigma_{\rm s}[\boldsymbol{f} - \boldsymbol{v}\cdot(\varepsilon\mathbf{1}+\mathbf{P})] + S_{\rm a}\boldsymbol{v}$$

CR vs. radiation hydrodynamics

- capitalize on analogies of CR and radiation hydrodynamics (Jiang & Oh 2018) derive two-moment equations from CR Vlasov equation (Thomas & CP 2019)
- lab-frame equ's for CR energy and momentum density, $\varepsilon_{\rm cr}$ and $\boldsymbol{f}_{\rm cr}/c^2$

$$\frac{\partial \varepsilon_{\rm cr}}{\partial t} + \boldsymbol{\nabla}\cdot\boldsymbol{f}_{\rm cr} = -\boldsymbol{w}_\pm \cdot \frac{\boldsymbol{bb}}{3\kappa_\pm}\cdot[\boldsymbol{f}_{\rm cr} - \boldsymbol{w}_\pm(\varepsilon_{\rm cr}+P_{\rm cr})] - \boldsymbol{v}\cdot\boldsymbol{g}_{\rm Lorentz} + S_\varepsilon$$

$$\frac{1}{c^2}\frac{\partial \boldsymbol{f}_{\rm cr}}{\partial t} + \boldsymbol{\nabla}\cdot\mathbf{P}_{\rm cr} = -\frac{\boldsymbol{bb}}{3\kappa_\pm}\cdot[\boldsymbol{f}_{\rm cr} - \boldsymbol{w}_\pm(\varepsilon_{\rm cr}+P_{\rm cr})] - \boldsymbol{g}_{\rm Lorentz} + \boldsymbol{S}_f$$

Alfvén wave velocity in lab frame: $\boldsymbol{w}_\pm = \boldsymbol{v} \pm \boldsymbol{v}_{\rm a}$,
CR scattering frequency $\bar{\nu}_\pm = c^2/(3\kappa_\pm)$

- lab-frame equ's for radiation energy and momentum density, ε and $\boldsymbol{f}/c^2$

(Mihalas & Mihalas, 1984, Lowrie+ 1999):

$$\frac{\partial \varepsilon}{\partial t} + \boldsymbol{\nabla}\cdot\boldsymbol{f} = -\sigma_{\rm s}\boldsymbol{v}\cdot[\boldsymbol{f} - \boldsymbol{v}\cdot(\varepsilon\mathbf{1}+\mathbf{P})] + S_{\rm a}$$

$$\frac{1}{c^2}\frac{\partial \boldsymbol{f}}{\partial t} + \boldsymbol{\nabla}\cdot\mathbf{P} = -\sigma_{\rm s}[\boldsymbol{f} - \boldsymbol{v}\cdot(\varepsilon\mathbf{1}+\mathbf{P})] + S_{\rm a}\boldsymbol{v}$$

- ***problem:*** *CR lab-frame equation requires resolving rapid gyrokinetics!*

CR vs. radiation hydrodynamics

- capitalize on analogies of CR and radiation hydrodynamics (Jiang & Oh 2018) derive two-moment equations from CR Vlasov equation (Thomas & CP 2019)
- lab-frame equ's for CR energy and momentum density, $\varepsilon_{\rm cr}$ and $\boldsymbol{f}_{\rm cr}/c^2$

$$\frac{\partial \varepsilon_{\rm cr}}{\partial t} + \boldsymbol{\nabla}\cdot\boldsymbol{f}_{\rm cr} = -\boldsymbol{w}_\pm \cdot \frac{\boldsymbol{bb}}{3\kappa_\pm}\cdot[\boldsymbol{f}_{\rm cr} - \boldsymbol{w}_\pm(\varepsilon_{\rm cr}+P_{\rm cr})] - \boldsymbol{v}\cdot\boldsymbol{g}_{\rm Lorentz} + S_\varepsilon$$

$$\frac{1}{c^2}\frac{\partial \boldsymbol{f}_{\rm cr}}{\partial t} + \boldsymbol{\nabla}\cdot\mathbf{P}_{\rm cr} = -\frac{\boldsymbol{bb}}{3\kappa_\pm}\cdot[\boldsymbol{f}_{\rm cr} - \boldsymbol{w}_\pm(\varepsilon_{\rm cr}+P_{\rm cr})] - \boldsymbol{g}_{\rm Lorentz} + \boldsymbol{S}_f$$

  Alfvén wave velocity in lab frame: $\boldsymbol{w}_\pm = \boldsymbol{v} \pm \boldsymbol{v}_{\rm a}$,
  CR scattering frequency $\bar{\nu}_\pm = c^2/(3\kappa_\pm)$
- lab-frame equ's for radiation energy and momentum density, ε and $\boldsymbol{f}/c^2$ (Mihalas & Mihalas, 1984, Lowrie+ 1999):

$$\frac{\partial \varepsilon}{\partial t} + \boldsymbol{\nabla}\cdot\boldsymbol{f} = -\sigma_{\rm s}\boldsymbol{v}\cdot[\boldsymbol{f} - \boldsymbol{v}\cdot(\varepsilon\mathbf{1}+\mathbf{P})] + S_{\rm a}$$

$$\frac{1}{c^2}\frac{\partial \boldsymbol{f}}{\partial t} + \boldsymbol{\nabla}\cdot\mathbf{P} = -\sigma_{\rm s}[\boldsymbol{f} - \boldsymbol{v}\cdot(\varepsilon\mathbf{1}+\mathbf{P})] + S_{\rm a}\boldsymbol{v}$$

- ***solution:*** *transform in comoving frame and project out gyrokinetics!*

Non-equilibrium CR streaming and diffusion

Coupling the evolution of CR and Alfvén wave energy densities

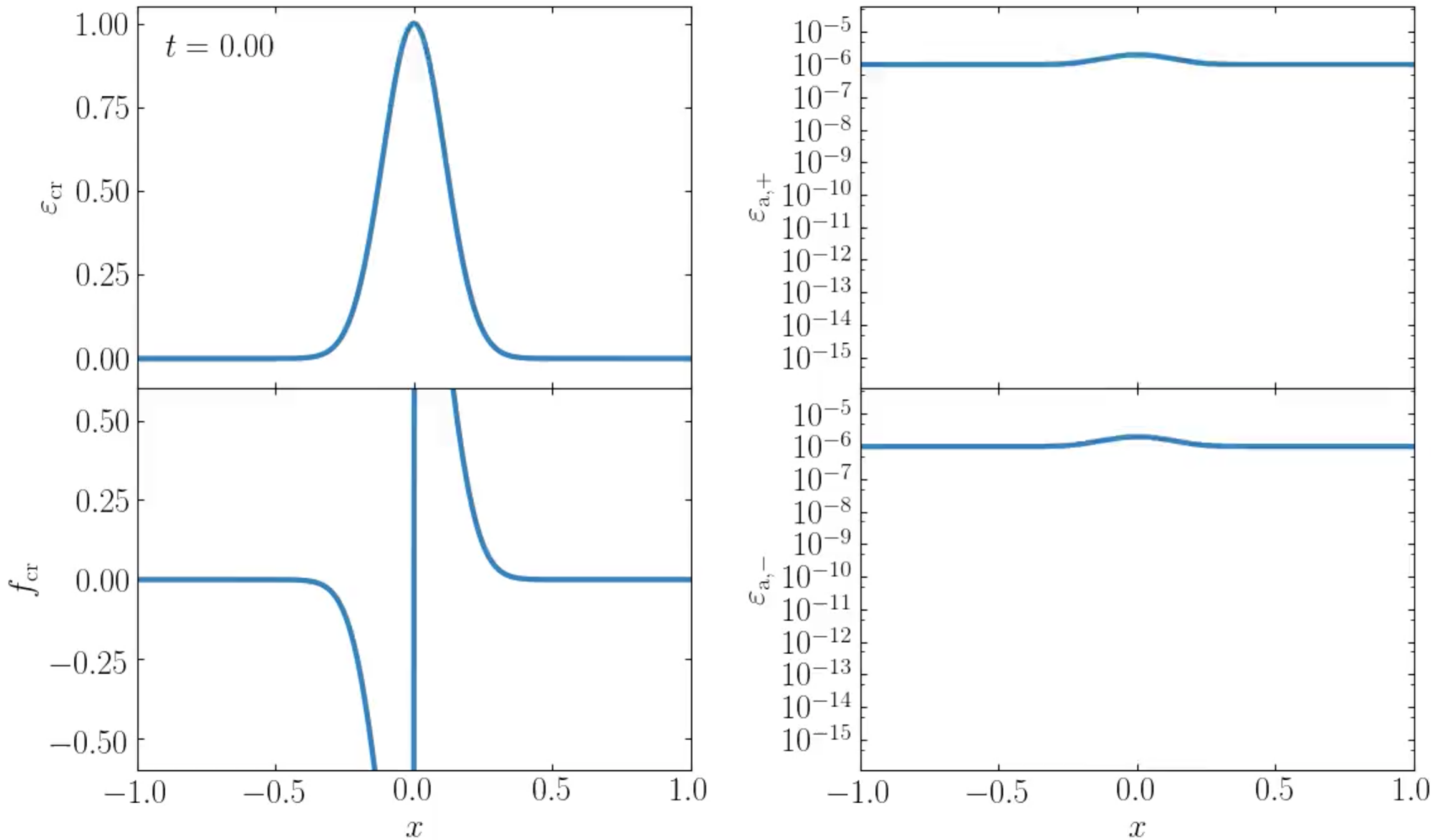

Thomas & CP (2019)

Non-equilibrium CR streaming and diffusion

Varying damping rate of Alfvén waves modulates the diffusivity of solution

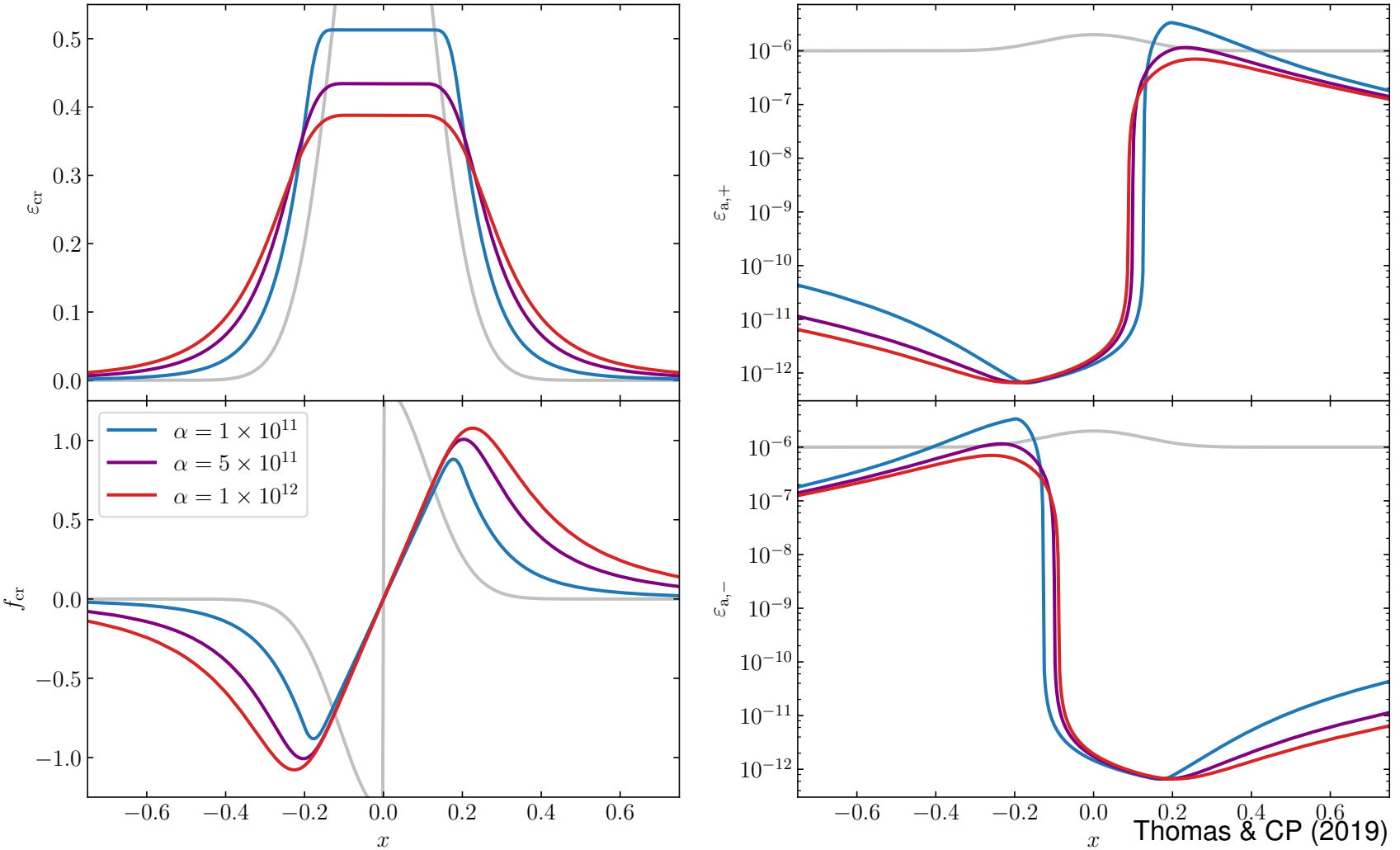

Thomas & CP (2019)

Anisotropic CR streaming and diffusion – AREPO

CR transport mediated by Alfvén waves and coupled to magneto-hydrodynamics

- CR streaming and diffusion along magnetic field lines in the self-confinement picture
- moment expansion similar to radiation hydrodynamics
- accounts for kinetic physics: non-linear Landau damping, gyro-resonant instability, ...
- Galilean invariant and causal transport
- energy and momentum conserving

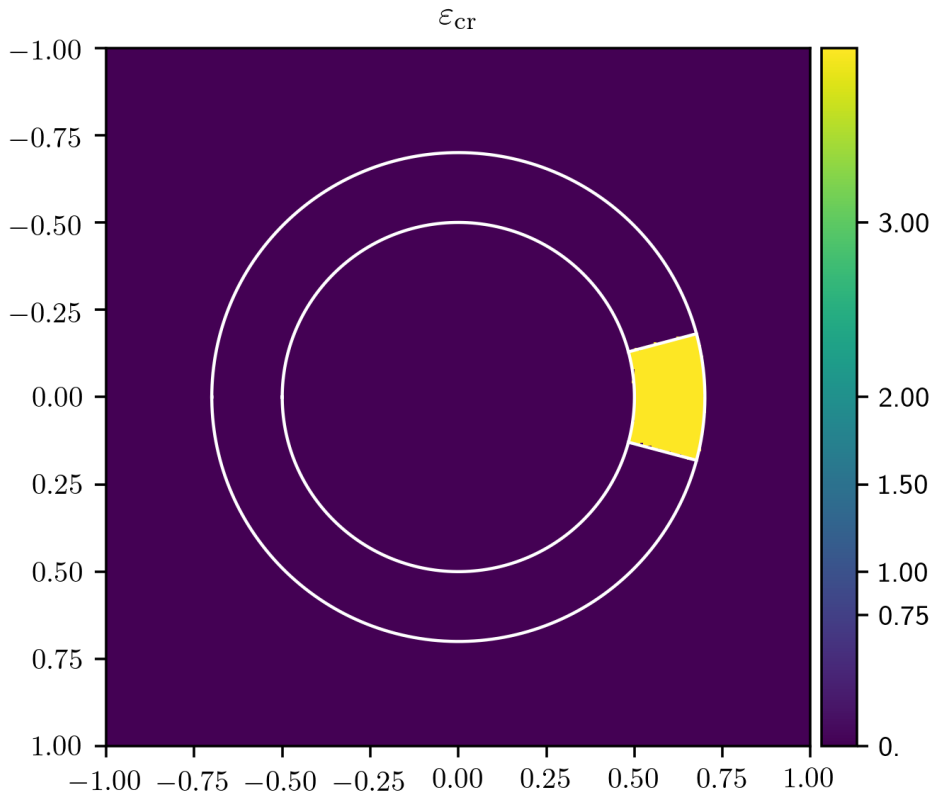

Thomas, Pakmor, CP (in prep.)

AIP

MeerKAT image of the Galactic Center

Haywood+ (Nature, 2019)

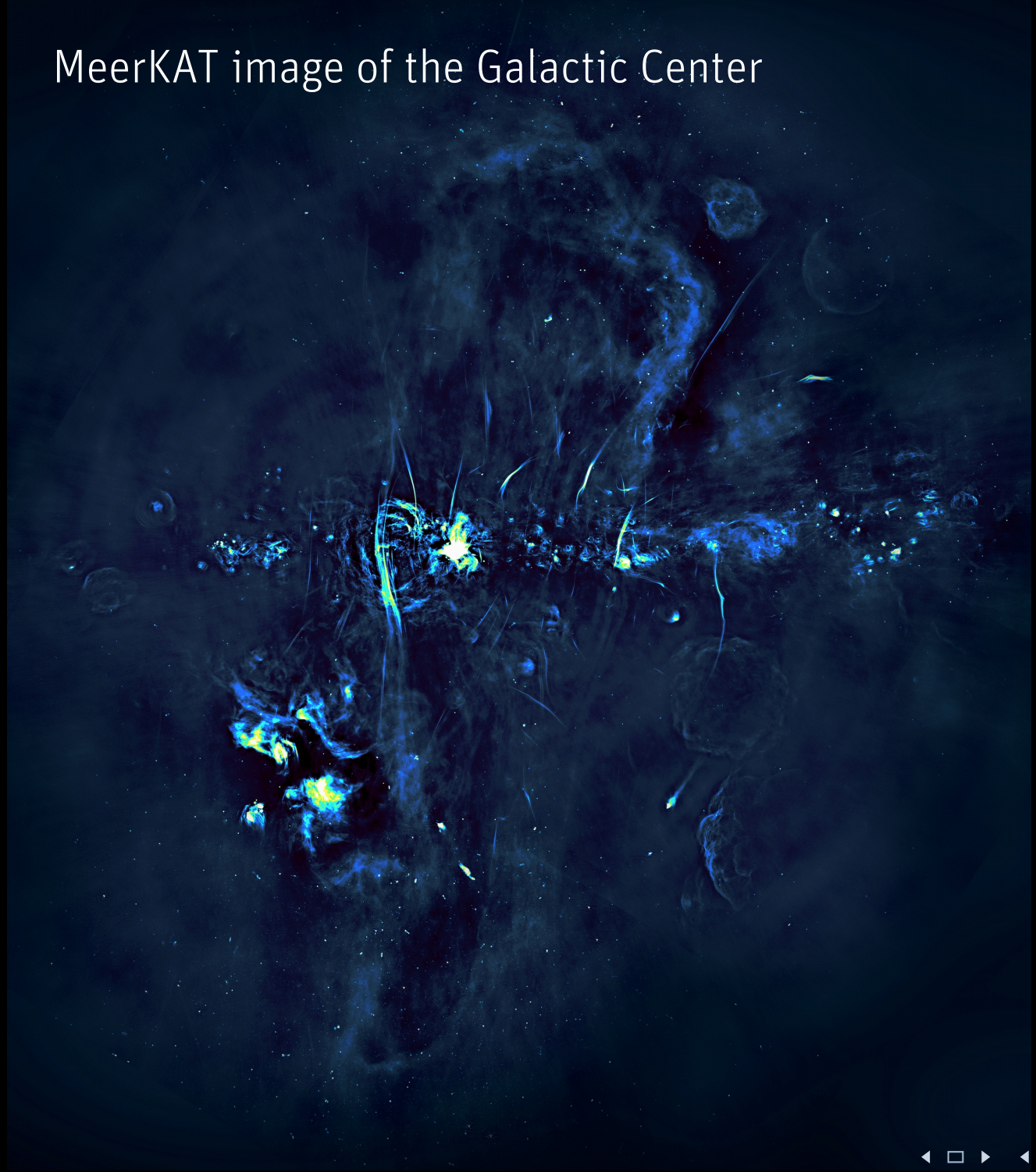

MeerKAT image of the Galactic Center

Haywood+ (Nature, 2019)

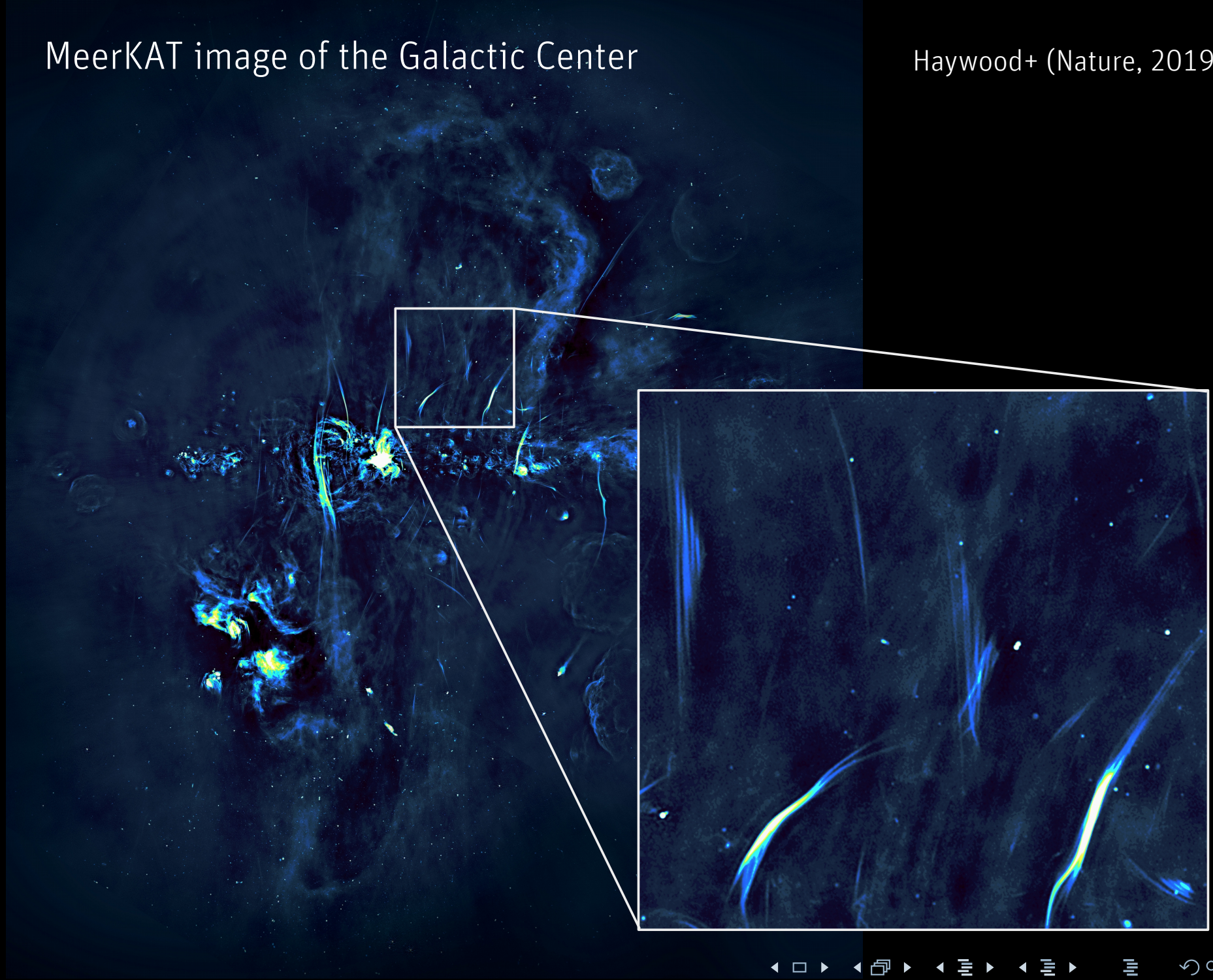

Radio synchrotron harps: the model

shock acceleration scenario

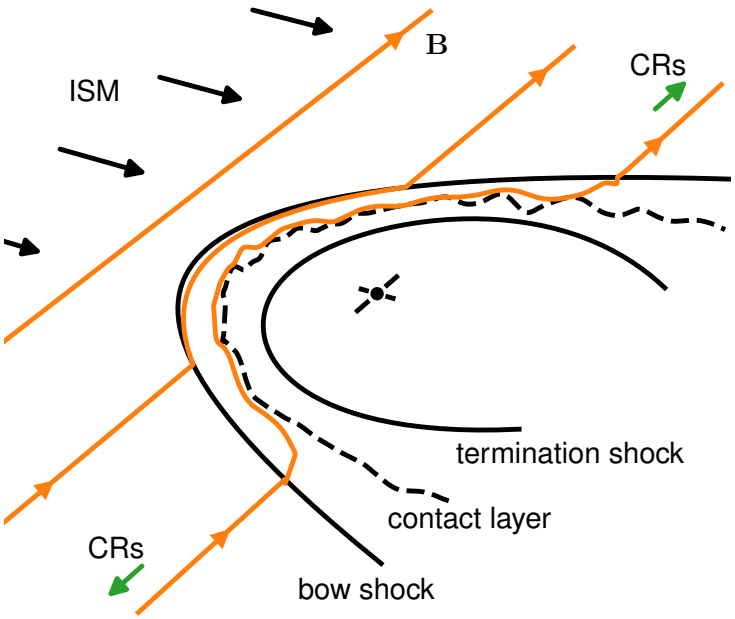

Thomas, CP, Enßlin (2020)

Radio synchrotron harps: the model

shock acceleration scenario

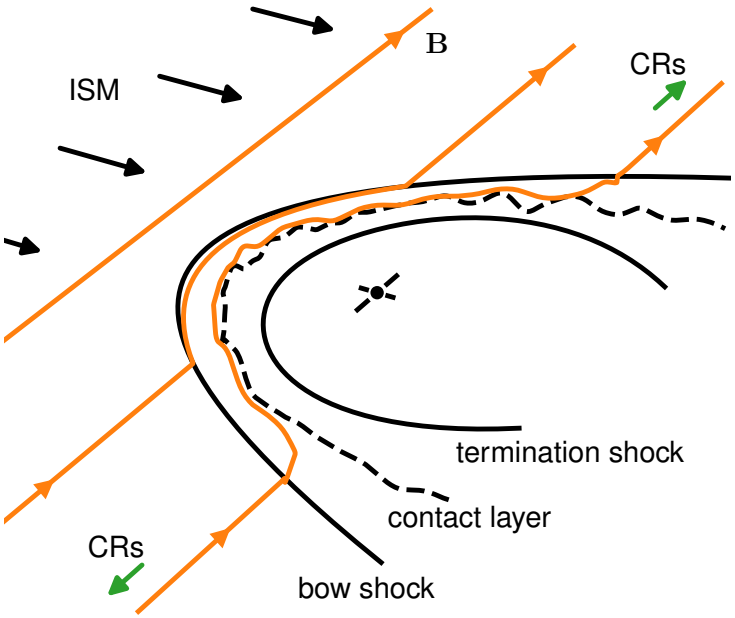

magnetic reconnection at pulsar wind

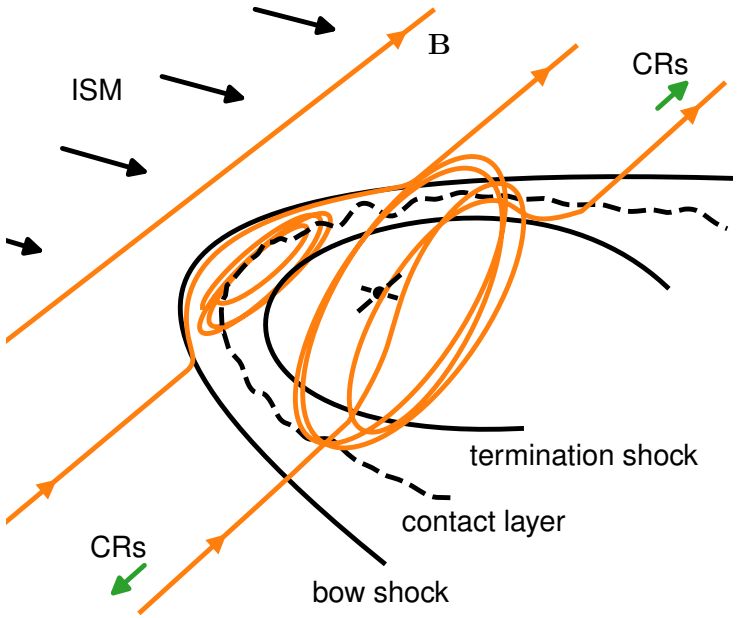

Thomas, CP, Enßlin (2020)

Radio synchrotron harps: the model

shock acceleration scenario

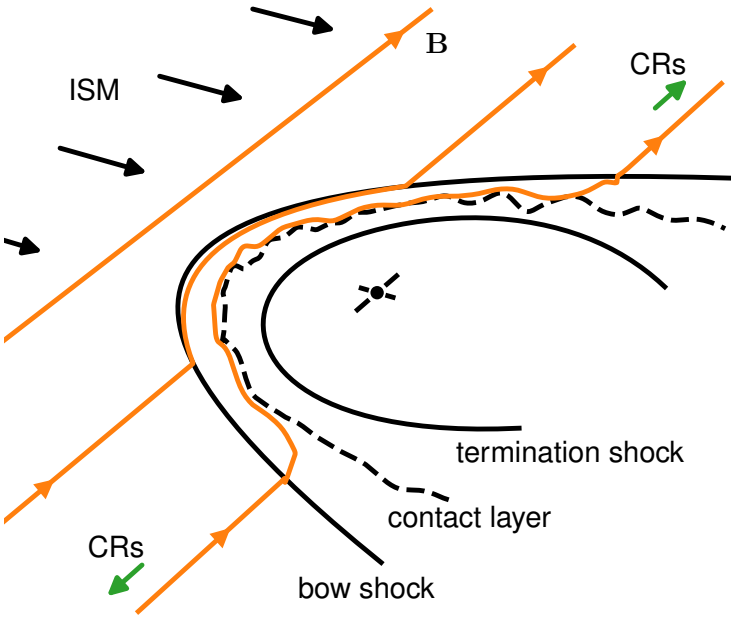

CR diffusion vs. streaming + diffusion

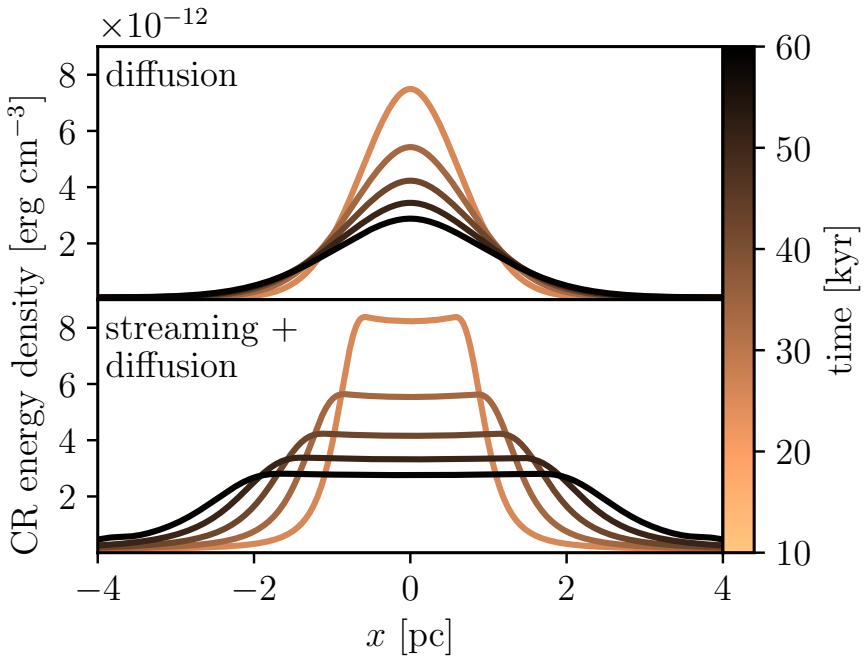

Thomas, CP, Enßlin (2020)

Radio synchrotron harps: testing CR propagation

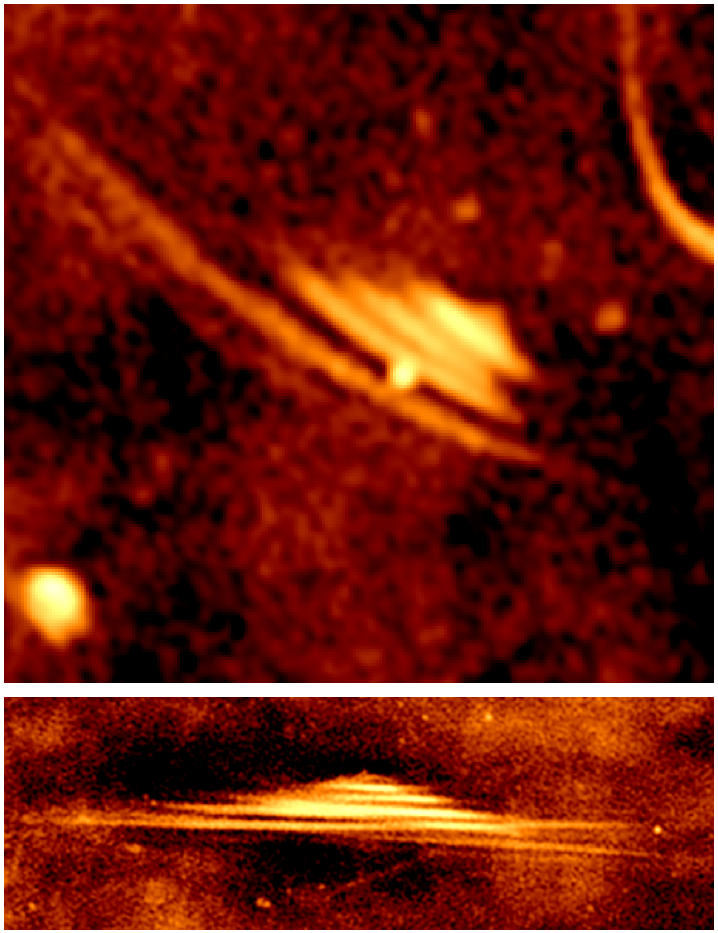

Haywood+ (Nature, 2019)

Radio synchrotron harps: testing CR propagation

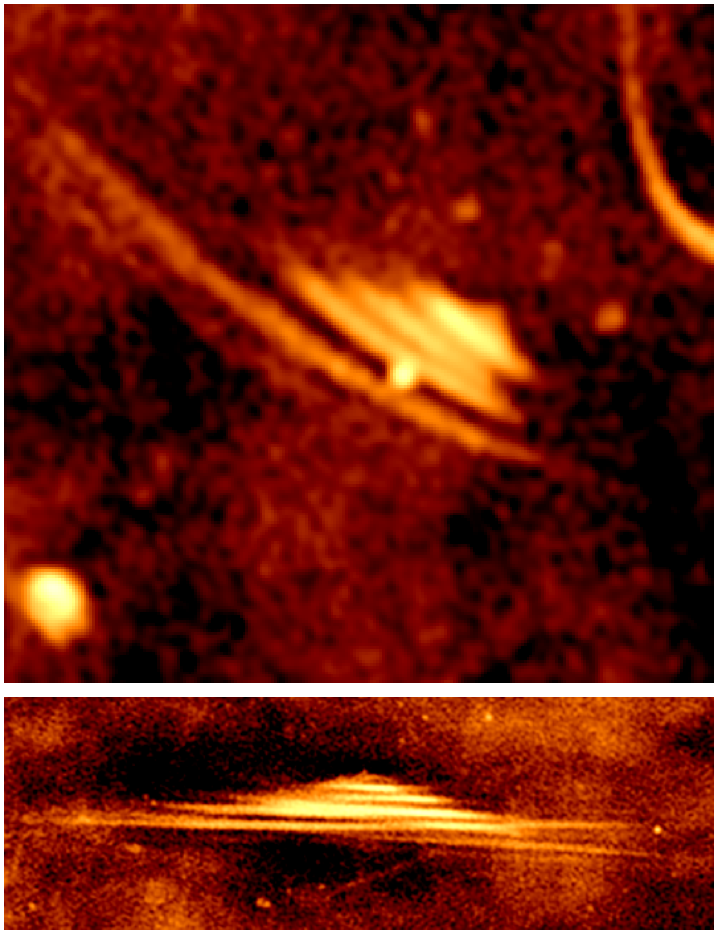

Haywood+ (Nature, 2019)

lateral radio profiles

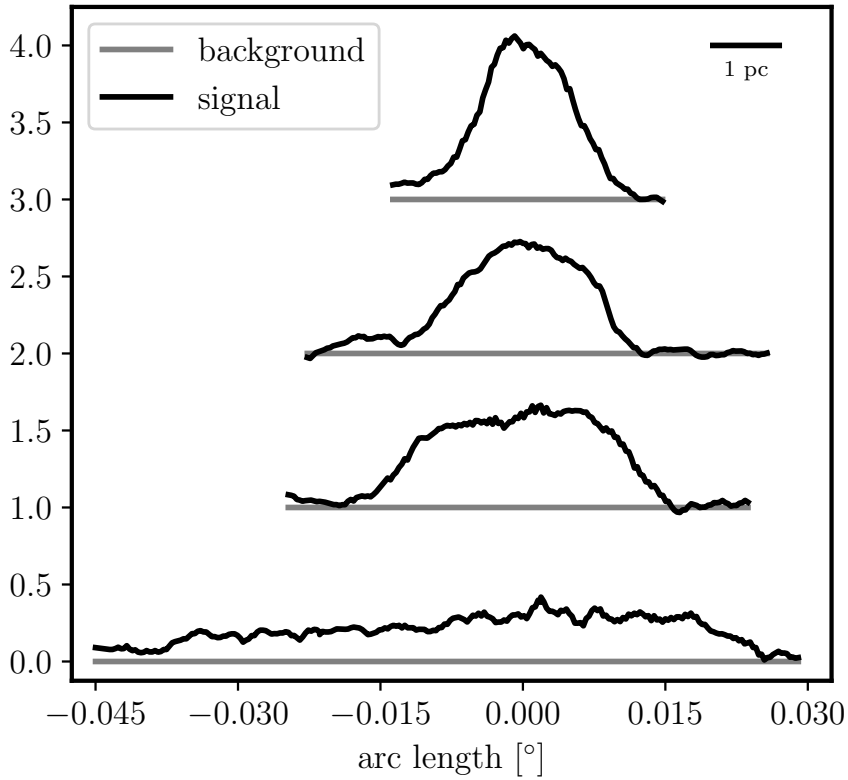

Thomas, CP, Enßlin (2020)

AIP

Radio synchrotron harps: testing CR propagation

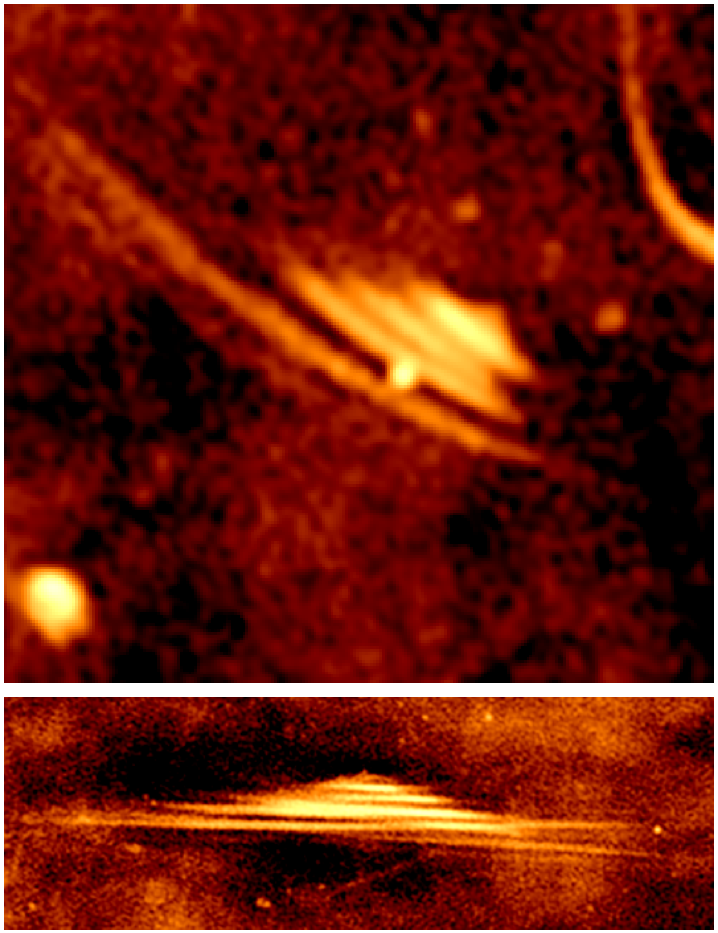

Haywood+ (Nature, 2019)

CR diffusion

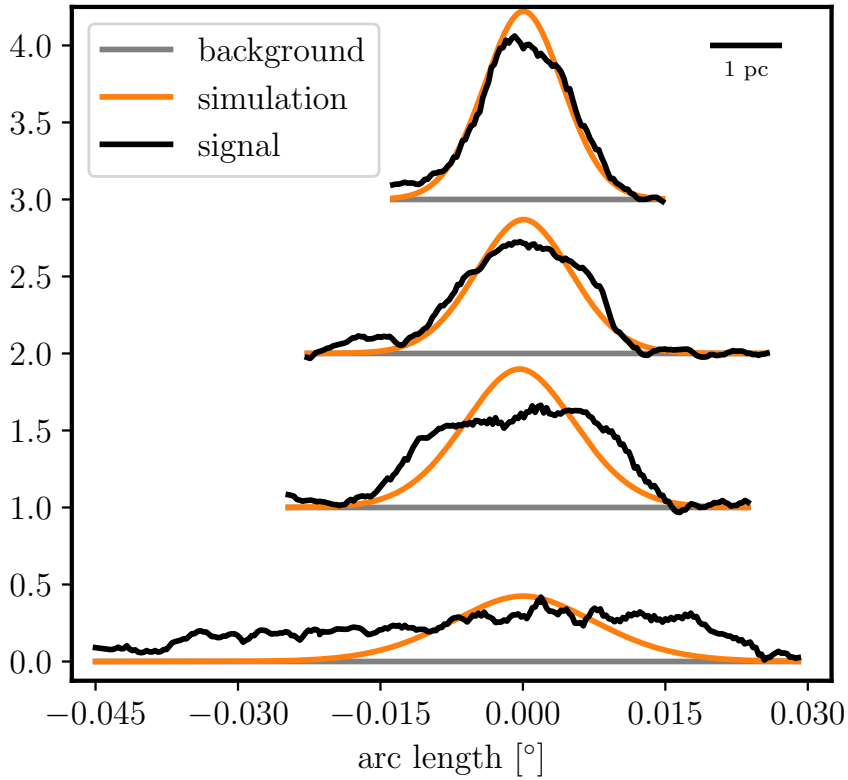

Thomas, CP, Enßlin (2020)

Radio synchrotron harps: testing CR propagation

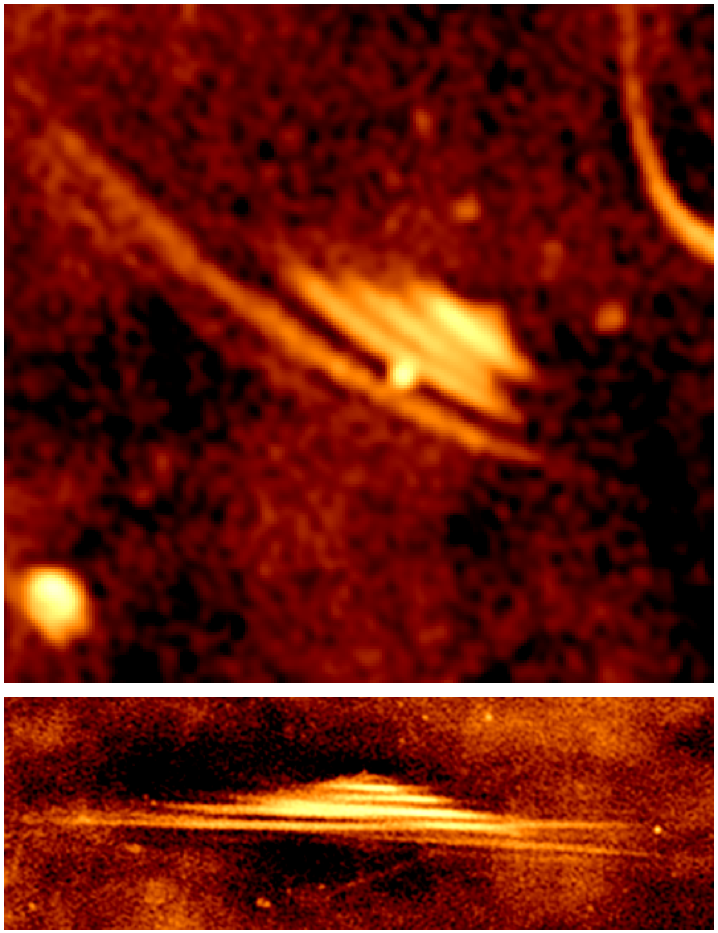

Haywood+ (Nature, 2019)

CR streaming and diffusion

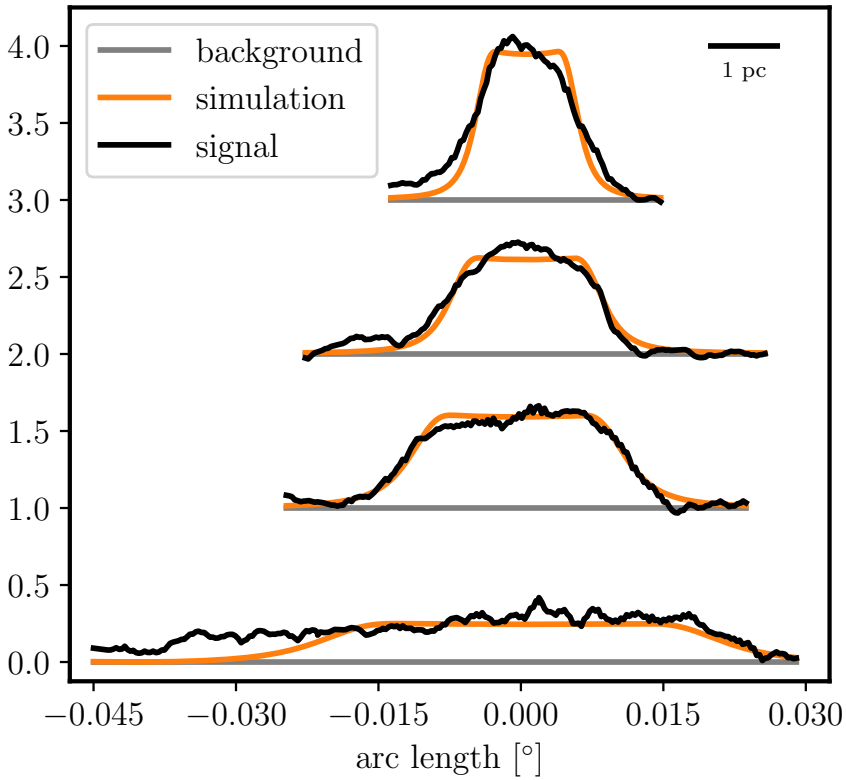

Thomas, CP, Enßlin (2020)

Conclusions for cosmic ray physics in galaxies

CR acceleration:

- TeV shell-type SNRs probe magnetic coherence scale in ISM
- hybrid-PIC simulations of p^+ acceleration agree with global SNR simulations
- global SNR simulations imply preferred quasi-parallel e^+ acceleration, more work needed for PIC sim's of e^- acceleration

Conclusions for cosmic ray physics in galaxies

CR acceleration:

- TeV shell-type SNRs probe magnetic coherence scale in ISM
- hybrid-PIC simulations of p^+ acceleration agree with global SNR simulations
- global SNR simulations imply preferred quasi-parallel e^+ acceleration, more work needed for PIC sim's of e^- acceleration

CR hydrodynamics:

- moment expansion similar to radiation hydrodynamics
- novel theory of CR transport mediated by Alfvén waves and coupled to magneto-hydrodynamics
- synchrotron harps: CR streaming dominates over diffusion

CRAGSMAN: The Impact of Cosmic RAys on Galaxy and CluSter ForMAtioN

This project has received funding from the European Research Counsil (ERC) under the European Union's Horizon 2020 research and innovation program (grant agreement No CRAGSMAN–646955).

AIP

Literature for the talk – 1

Cosmic ray acceleration:

- Pais, Pfrommer, Ehlert, Pakmor, *The effect of cosmic-ray acceleration on supernova blast wave dynamics,* 2018, MNRAS, 478, 5278.
- Winner, Pfrommer, Girichidis, Pakmor, *Evolution of cosmic ray electron spectra in magnetohydrodynamical simulations,* 2019, MNRAS, 488, 2235.
- Pais, Pfrommer, Ehlert, Werhahn, Winner, *Constraining the coherence scale of the interstellar magnetic field using TeV gamma-ray observations of supernova remnants,* 2020, MNRAS, 496, 2448.
- Pais, Pfrommer, *Simulating TeV gamma-ray morphologies of shell-type supernova remnants,* 2020, MNRAS, 498, 5557.
- Winner, Pfrommer, Girichidis, Werhahn, Pais, *Evolution and observational signatures of the cosmic ray electron spectrum in SN 1006,* 2020, MNRAS, 499, 2785.

Literature for the talk – 2

Cosmic ray hydrodynamics:

- Pfrommer, Pakmor, Schaal, Simpson, Springel, *Simulating cosmic ray physics on a moving mesh,* 2017, MNRAS, 465, 4500.
- Thomas & Pfrommer, *Cosmic-ray hydrodynamics: Alfvén-wave regulated transport of cosmic rays,* 2019, MNRAS, 485, 2977.
- Thomas, Pfrommer, Enßlin, *Probing cosmic ray transport with radio synchrotron harps in the Galactic center,* 2020, ApJL, 890, L18.
- Thomas, Pfrommer, Pakmor, *A finite volume method for two-moment cosmic-ray hydrodynamics on a moving mesh,* 2021, submitted